Upper Limits on the Isotropic Gravitational-Wave Background from the first part of LIGO, Virgo, and KAGRA's fourth Observing Run

The LIGO Scientific Collaboration, The Virgo Collaboration, and The KAGRA Collaboration

A. G. Abac,[1] I. Abouelfettouh,[2] F. Acernese,[3,4] K. Ackley,[5] C. Adamcewicz,[6] S. Adhicary,[7] D. Adhikari,[8,9] N. Adhikari,[10] R. X. Adhikari,[11] V. K. Adkins,[12] S. Afroz,[13] A. Agapito,[14] D. Agarwal,[15] M. Agathos,[16] N. Aggarwal,[17] S. Aggarwal,[18] O. D. Aguiar,[19] I.-L. Ahrend,[20] L. Aiello,[21,22] A. Ain,[23] P. Ajith,[24] T. Akutsu,[25,26] S. Albanesi,[27,28] W. Ali,[29,30] S. Al-Kershi,[8,9] C. Alléné,[31] A. Allocca,[32,4] S. Al-Shammari,[33] P. A. Altin,[34] S. Alvarez-Lopez,[35] W. Amar,[31] O. Amarasinghe,[33] A. Amato,[36,37] F. Amicucci,[38,39] C. Amra,[40] A. Ananyeva,[11] S. B. Anderson,[11] W. G. Anderson,[11] M. Andia,[41] M. Ando,[42] M. Andrés-Carcasona,[43] T. Andrić,[44,45,8,9] J. Anglin,[46] S. Ansoldi,[47,48] J. M. Antelis,[49] S. Antier,[41] M. Aoumi,[50] E. Z. Appavuravther,[51,52] S. Appert,[11] S. K. Apple,[53] K. Arai,[11] A. Araya,[42] M. C. Araya,[11] M. Arca Sedda,[44,45] J. S. Areeda,[54] N. Aritomi,[2] F. Armato,[29,30] S. Armstrong,[55] N. Arnaud,[56] M. Arogeti,[57] S. M. Aronson,[12] G. Ashton,[58] Y. Aso,[25,59] L. Asprea,[28] M. Assiduo,[60,61] S. Assis de Souza Melo,[62] S. M. Aston,[63] P. Astone,[38] F. Attadio,[39,38] F. Aubin,[64] K. AultONeal,[65] G. Avallone,[66] E. A. Avila,[49] S. Babak,[20] C. Badger,[67] S. Bae,[68] S. Bagnasco,[28] L. Baiotti,[69] R. Bajpai,[70] T. Baka,[71,37] A. M. Baker,[6] K. A. Baker,[72] T. Baker,[73] G. Baldi,[74,75] N. Baldicchi,[76,51] M. Ball,[77] G. Ballardin,[62] S. W. Ballmer,[78] S. Banagiri,[6] B. Banerjee,[44] D. Bankar,[79] T. M. Baptiste,[12] P. Baral,[10] M. Baratti,[80,81] J. C. Barayoga,[11] B. C. Barish,[11] D. Barker,[2] N. Barman,[79] P. Barneo,[82,83,84] F. Barone,[85,4] B. Barr,[86] L. Barsotti,[35] M. Barsuglia,[20] D. Barta,[87] A. M. Bartoletti,[88] M. A. Barton,[86] I. Bartos,[46] A. Basalaev,[8,9] R. Bassiri,[89] A. Basti,[81,80] M. Bawaj,[76,51] P. Baxi,[90] J. C. Bayley,[86] A. C. Baylor,[10] P. A. Baynard II,[57] M. Bazzan,[91,92] V. M. Bedakihale,[93] F. Beirnaert,[94] M. Bejger,[95] D. Belardinelli,[22] A. S. Bell,[86] D. S. Bellie,[96] L. Bellizzi,[80,81] W. Benoit,[18] I. Bentara,[56] J. D. Bentley,[97] M. Ben Yaala,[55] S. Bera,[98,99] F. Bergamin,[33] B. K. Berger,[89] S. Bernuzzi,[27] M. Beroiz,[11] D. Bersanetti,[29] T. Bertheas,[100] A. Bertolini,[37,36] J. Betzwieser,[63] D. Beveridge,[72] G. Bevilacqua,[101] N. Bevins,[102] R. Bhandare,[103] R. Bhatt,[11] D. Bhattacharjee,[104,105] S. Bhattacharyya,[106] S. Bhaumik,[46] V. Biancalana,[101] A. Bianchi,[37,107] I. A. Bilenko,[108] G. Billingsley,[11] A. Binetti,[109] S. Bini,[11,74,75] C. Binu,[110] S. Biot,[111] O. Birnholtz,[112] S. Biscoveanu,[96] A. Bisht,[9] M. Bitossi,[62,80] M.-A. Bizouard,[113] S. Blaber,[114] J. K. Blackburn,[11] L. A. Blagg,[77] C. D. Blair,[72,63] D. G. Blair,[72] N. Bode,[8,9] N. Boettner,[97] G. Boileau,[113] M. Boldrini,[38] G. N. Bolingbroke,[115] A. Bolliand,[116,40] L. D. Bonavena,[46] R. Bondarescu,[82] F. Bondu,[117] E. Bonilla,[89] M. S. Bonilla,[54] A. Bonino,[118] R. Bonnand,[31,116] A. Borchers,[8,9] S. Borhanian,[7] V. Boschi,[80] S. Bose,[119] V. Bossilkov,[63] Y. Bothra,[37,107] A. Boudon,[56] L. Bourg,[57] G. Bouyer,[120] M. Boyle,[121] A. Bozzi,[62] C. Bradaschia,[80] P. R. Brady,[10] A. Branch,[63] M. Branchesi,[44,45] I. Braun,[104] T. Briant,[122] A. Brillet,[113] M. Brinkmann,[8,9] P. Brockill,[10] E. Brockmueller,[8,9] A. F. Brooks,[11] B. C. Brown,[46] D. D. Brown,[115] M. L. Brozzetti,[76,51] S. Brunett,[11] G. Bruno,[15] R. Bruntz,[123] J. Bryant,[118] Y. Bu,[124] F. Bucci,[61] J. Buchanan,[123] O. Bulashenko,[82,83] T. Bulik,[125] H. J. Bulten,[37] A. Buonanno,[126,1] K. Burtnyk,[2] R. Buscicchio,[127,128] D. Buskulic,[31] C. Buy,[100] R. L. Byer,[89] G. S. Cabourn Davies,[73] R. Cabrita,[15] V. Cáceres-Barbosa,[7] L. Cadonati,[57] G. Cagnoli,[129] C. Cahillane,[78] A. Calafat,[98] T. A. Callister,[130] E. Calloni,[32,4] S. R. Callos,[77] G. Caneva Santoro,[43] K. C. Cannon,[42] H. Cao,[35] L. A. Capistran,[131] E. Capocasa,[20] E. Capote,[2,11] G. Capurri,[81,80] G. Carapella,[66,132] F. Carbognani,[62] M. Carlassara,[8,9] J. B. Carlin,[124] T. K. Carlson,[133] M. F. Carney,[104] M. Carpinelli,[127,62] G. Carrillo,[77] J. J. Carter,[8,9] G. Carullo,[118,134] A. Casallas-Lagos,[135] J. Casanueva Diaz,[62] C. Casentini,[136,22] S. Y. Castro-Lucas,[137] S. Caudill,[133] M. Cavaglià,[105] R. Cavalieri,[62] A. Ceja,[54] G. Cella,[80] P. Cerdá-Durán,[138,139] E. Cesarini,[22] N. Chabbra,[34] W. Chaibi,[113] A. Chakraborty,[13] P. Chakraborty,[8,9] S. Chakraborty,[103] S. Chalathadka Subrahmanya,[97] J. C. L. Chan,[140] M. Chan,[114] K. Chang,[141] S. Chao,[142,141] P. Charlton,[143] E. Chassande-Mottin,[20] C. Chatterjee,[144] Debarati Chatterjee,[79] Deep Chatterjee,[35] M. Chaturvedi,[103] S. Chaty,[20] K. Chatziioannou,[11] A. Chen,[145] A. H.-Y. Chen,[146] D. Chen,[147] H. Chen,[142] H. Y. Chen,[120] S. Chen,[144] Yanbei Chen,[148] Yitian Chen,[121] H. P. Cheng,[149] P. Chessa,[76,51] H. T. Cheung,[90] S. Y. Cheung,[6] F. Chiadini,[150,132] G. Chiarini,[8,9,92] A. Chiba,[151] A. Chincarini,[29] M. L. Chiofalo,[81,80] A. Chiummo,[4,62] C. Chou,[146] S. Choudhary,[72] N. Christensen,[113,152] S. S. Y. Chua,[34] G. Ciani,[74,75] P. Ciecielag,[95] M. Cieślar,[125] M. Cifaldi,[22] B. Cirok,[153] F. Clara,[2] J. A. Clark,[11,57] T. A. Clarke,[6] P. Clearwater,[154] S. Clesse,[111] F. Cleva,[113,116] E. Coccia,[44,45,43] E. Codazzo,[155,156] P.-F. Cohadon,[122] S. Colace,[30] E. Colangeli,[73] M. Colleoni,[98] C. G. Collette,[157] J. Collins,[63] S. Colloms,[86] A. Colombo,[158,128]

C. M. Compton,[2] G. Connolly,[77] L. Conti,[92] T. R. Corbitt,[12] I. Cordero-Carrión,[159] S. Corezzi,[76,51] N. J. Cornish,[160] I. Coronado,[161] A. Corsi,[162] R. Cottingham,[63] M. W. Coughlin,[18] A. Couineaux,[38] P. Couvares,[11,57] D. M. Coward,[72] R. Coyne,[163] A. Cozzumbo,[44] J. D. E. Creighton,[10] T. D. Creighton,[164] P. Cremonese,[98] S. Crook,[63] R. Crouch,[2] J. Csizmazia,[2] J. R. Cudell,[165] T. J. Cullen,[11] A. Cumming,[86] E. Cuoco,[166,167] M. Cusinato,[138] L. V. Da Conceição,[168] T. Dal Canton,[41] S. Dal Pra,[169] G. Dálya,[100] B. D'Angelo,[29] S. Danilishin,[36,37] S. D'Antonio,[38] K. Danzmann,[9,8,9] K. E. Darroch,[123] L. P. Dartez,[63] R. Das,[106] A. Dasgupta,[93] V. Dattilo,[62] A. Daumas,[20] N. Davari,[170,171] I. Dave,[103] A. Davenport,[137] M. Davier,[41] T. F. Davies,[72] D. Davis,[11] L. Davis,[72] M. C. Davis,[18] P. Davis,[172,173] E. J. Daw,[174] M. Dax,[1] J. De Bolle,[94] M. Deenadayalan,[79] J. Degallaix,[175] M. De Laurentis,[32,4] F. De Lillo,[23] S. Della Torre,[128] W. Del Pozzo,[81,80] A. Demagny,[31] F. De Marco,[39,38] G. Demasi,[176,61] F. De Matteis,[21,22] N. Demos,[35] T. Dent,[177] A. Depasse,[15] N. DePergola,[102] R. De Pietri,[178,179] R. De Rosa,[32,4] C. De Rossi,[62] M. Desai,[35] R. DeSalvo,[180] A. DeSimone,[181] R. De Simone,[150,132] A. Dhani,[1] R. Diab,[46] M. C. Díaz,[164] M. Di Cesare,[32,4] G. Dideron,[182] T. Dietrich,[1] L. Di Fiore,[4] C. Di Fronzo,[72] M. Di Giovanni,[39,38] T. Di Girolamo,[32,4] D. Diksha,[37,36] J. Ding,[20,183] S. Di Pace,[39,38] I. Di Palma,[39,38] D. Di Piero,[184,48] F. Di Renzo,[56] Divyajyoti,[33] A. Dmitriev,[118] J. P. Docherty,[86] Z. Doctor,[96] N. Doerksen,[168] E. Dohmen,[2] A. Doke,[133] A. Domiciano De Souza,[185] L. D'Onofrio,[38] F. Donovan,[35] K. L. Dooley,[33] T. Dooney,[71] S. Doravari,[79] O. Dorosh,[186] W. J. D. Doyle,[123] M. Drago,[39,38] J. C. Driggers,[2] L. Dunn,[124] U. Dupletsa,[44] D. D'Urso,[170,155] P. Dutta Roy,[46] H. Duval,[187] S. E. Dwyer,[2] C. Eassa,[2] M. Ebersold,[188,31] T. Eckhardt,[97] G. Eddolls,[78] A. Effler,[63] J. Eichholz,[34] H. Einsle,[113] M. Eisenmann,[25] M. Emma,[58] K. Endo,[151] R. Enficiaud,[1] L. Errico,[32,4] R. Espinosa,[164] M. C. Espitia,[189] M. Esposito,[4,32] R. C. Essick,[190] H. Estellés,[1] T. Etzel,[11] M. Evans,[35] T. Evstafyeva,[182] B. E. Ewing,[7] J. M. Ezquiaga,[140] F. Fabrizi,[60,61] V. Fafone,[21,22] S. Fairhurst,[33] A. M. Farah,[130] B. Farr,[77] W. M. Farr,[191,192] G. Favaro,[91] M. Favata,[193] M. Fays,[165] M. Fazio,[55] J. Feicht,[11] M. M. Fejer,[89] R. Felicetti,[184,48] E. Fenyvesi,[87,194] J. Fernandes,[195] T. Fernandes,[196,138] D. Fernando,[110] S. Ferraiuolo,[197,39,38] T. A. Ferreira,[12] F. Fidecaro,[81,80] P. Figura,[95] A. Fiori,[80,81] I. Fiori,[62] M. Fishbach,[190] R. P. Fisher,[123] R. Fittipaldi,[198,132] V. Fiumara,[199,132] R. Flaminio,[31] S. M. Fleischer,[200] L. S. Fleming,[201] E. Floden,[18] H. Fong,[114] J. A. Font,[138,139] F. Fontinele-Nunes,[18] C. Foo,[1] B. Fornal,[202] K. Franceschetti,[178] F. Frappez,[31] S. Frasca,[39,38] F. Frasconi,[80] J. P. Freed,[65] Z. Frei,[203] A. Freise,[37,107] O. Freitas,[196,138] R. Frey,[77] W. Frischhertz,[63] P. Fritschel,[35] V. V. Frolov,[63] G. G. Fronzé,[28] M. Fuentes-Garcia,[11] S. Fujii,[204] T. Fujimori,[205] P. Fulda,[46] M. Fyffe,[63] B. Gadre,[71] J. R. Gair,[1] S. Galaudage,[185] V. Galdi,[206] R. Gamba,[7] A. Gamboa,[1] S. Gamoji,[180] D. Ganapathy,[207] A. Ganguly,[79] B. Garaventa,[29] J. García-Bellido,[208] C. García-Quirós,[188] J. W. Gardner,[34] K. A. Gardner,[114] S. Garg,[42] J. Gargiulo,[62] X. Garrido,[41] A. Garron,[98] F. Garufi,[32,4] P. A. Garver,[89] C. Gasbarra,[21,22] B. Gateley,[2] F. Gautier,[209] V. Gayathri,[10] T. Gayer,[78] G. Gemme,[29] A. Gennai,[80] V. Gennari,[100] J. George,[103] R. George,[120] O. Gerberding,[97] L. Gergely,[153] Archisman Ghosh,[94] Sayantan Ghosh,[195] Shaon Ghosh,[193] Shrobana Ghosh,[8,9] Suprovo Ghosh,[210] Tathagata Ghosh,[79] J. A. Giaime,[12,63] K. D. Giardina,[63] D. R. Gibson,[201] C. Gier,[55] S. Gkaitatzis,[81,80] J. Glanzer,[11] F. Glotin,[41] J. Godfrey,[77] R. V. Godley,[8,9] P. Godwin,[11] A. S. Goettel,[33] E. Goetz,[114] J. Golomb,[11] S. Gomez Lopez,[39,38] B. Goncharov,[44] G. González,[12] P. Goodarzi,[211] S. Goode,[6] A. W. Goodwin-Jones,[15] M. Gosselin,[62] R. Gouaty,[31] D. W. Gould,[34] K. Govorkova,[35] A. Grado,[76,51] V. Graham,[86] A. E. Granados,[18] M. Granata,[175] V. Granata,[212,132] S. Gras,[35] P. Grassia,[11] J. Graves,[57] C. Gray,[2] R. Gray,[86] G. Greco,[51] A. C. Green,[37,107] L. Green,[213] S. M. Green,[73] S. R. Green,[214] C. Greenberg,[133] A. M. Gretarsson,[65] H. K. Griffin,[18] D. Griffith,[11] H. L. Griggs,[57] G. Grignani,[76,51] C. Grimaud,[31] H. Grote,[33] S. Grunewald,[1] D. Guerra,[138] D. Guetta,[215] G. M. Guidi,[60,61] A. R. Guimaraes,[12] H. K. Gulati,[93] F. Gulminelli,[172,173] H. Guo,[145] W. Guo,[72] Y. Guo,[37,36] Anuradha Gupta,[216] I. Gupta,[7] N. C. Gupta,[93] S. K. Gupta,[46] V. Gupta,[18] N. Gupte,[1] J. Gurs,[97] N. Gutierrez,[175] N. Guttman,[6] F. Guzman,[131] D. Haba,[217] M. Haberland,[1] S. Haino,[218] E. D. Hall,[35] E. Z. Hamilton,[98] G. Hammond,[86] M. Haney,[37] J. Hanks,[2] C. Hanna,[7] M. D. Hannam,[33] O. A. Hannuksela,[219] A. G. Hanselman,[130] H. Hansen,[2] J. Hanson,[63] S. Hanumasagar,[57] R. Harada,[42] A. R. Hardison,[181] S. Harikumar,[186] K. Haris,[37,71] I. Harley-Trochimczyk,[131] T. Harmark,[134] J. Harms,[44,45] G. M. Harry,[220] I. W. Harry,[73] J. Hart,[104] B. Haskell,[95,221,222] C. J. Haster,[213] K. Haughian,[86] H. Hayakawa,[50] K. Hayama,[223] M. C. Heintze,[63] J. Heinze,[118] J. Heinzel,[35] H. Heitmann,[113] F. Hellman,[207] A. F. Helmling-Cornell,[77] G. Hemming,[62] O. Henderson-Sapir,[115] M. Hendry,[86] I. S. Heng,[86] M. H. Hennig,[86] C. Henshaw,[57] M. Heurs,[8,9] A. L. Hewitt,[224,225] J. Heynen,[15]

J. Heyns,[35] S. Higginbotham,[33] S. Hild,[36,37] S. Hill,[86] Y. Himemoto,[226] N. Hirata,[25] C. Hirose,[227] D. Hofman,[175] B. E. Hogan,[65] N. A. Holland,[37,107] I. J. Hollows,[174] D. E. Holz,[130] L. Honet,[111] D. J. Horton-Bailey,[207] J. Hough,[86] S. Hourihane,[11] N. T. Howard,[144] E. J. Howell,[72] C. G. Hoy,[73] C. A. Hrishikesh,[21] P. Hsi,[35] H.-F. Hsieh,[142] H.-Y. Hsieh,[142] C. Hsiung,[228] S.-H. Hsu,[146] W.-F. Hsu,[109] Q. Hu,[86] H. Y. Huang,[141] Y. Huang,[7] Y. T. Huang,[78] A. D. Huddart,[229] B. Hughey,[65] V. Hui,[31] S. Husa,[98] R. Huxford,[7] L. Iampieri,[39,38] G. A. Iandolo,[36] M. Ianni,[22,21] G. Iannone,[132] J. Iascau,[77] K. Ide,[230] R. Iden,[217] A. Ierardi,[44,45] S. Ikeda,[147] H. Imafuku,[42] Y. Inoue,[141] G. Iorio,[91] P. Iosif,[184,48] M. H. Iqbal,[34] J. Irwin,[86] R. Ishikawa,[230] M. Isi,[191,192] K. S. Isleif,[231] Y. Itoh,[205,232] M. Iwaya,[204] B. R. Iyer,[24] C. Jacquet,[100] P.-E. Jacquet,[122] T. Jacquot,[41] S. J. Jadhav,[233] S. P. Jadhav,[154] M. Jain,[133] T. Jain,[224] A. L. James,[11] K. Jani,[144] J. Janquart,[15] K. Janssens,[23] N. N. Janthalur,[233] S. Jaraba,[234] P. Jaranowski,[235] R. Jaume,[98] W. Javed,[33] A. Jennings,[2] M. Jensen,[2] W. Jia,[35] J. Jiang,[149] H.-B. Jin,[236,237] G. R. Johns,[123] N. A. Johnson,[46] M. C. Johnston,[213] R. Johnston,[86] N. Johny,[8,9] D. H. Jones,[34] D. I. Jones,[210] R. Jones,[86] H. E. Jose,[77] P. Joshi,[7] S. K. Joshi,[79] G. Joubert,[56] J. Ju,[238] L. Ju,[72] K. Jung,[239] J. Junker,[34] V. Juste,[111] H. B. Kabagoz,[63,35] T. Kajita,[240] I. Kaku,[205] V. Kalogera,[96] M. Kalomenopoulos,[213] M. Kamiizumi,[50] N. Kanda,[232,205] S. Kandhasamy,[79] G. Kang,[241] N. C. Kannachel,[6] J. B. Kanner,[11] S. A. KantiMahanty,[18] S. J. Kapadia,[79] D. P. Kapasi,[54] M. Karthikeyan,[133] M. Kasprzack,[11] H. Kato,[151] T. Kato,[204] E. Katsavounidis,[35] W. Katzman,[63] R. Kaushik,[103] K. Kawabe,[2] R. Kawamoto,[205] D. Keitel,[98] L. J. Kemperman,[115] J. Kennington,[7] F. A. Kerkow,[18] R. Kesharwani,[79] J. S. Key,[242] R. Khadela,[8,9] S. Khadka,[89] S. S. Khadkikar,[7] F. Y. Khalili,[108] F. Khan,[8,9] T. Khanam,[162] M. Khursheed,[103] N. M. Khusid,[191,192] W. Kiendrebeogo,[113,243] N. Kijbunchoo,[115] C. Kim,[244] J. C. Kim,[245] K. Kim,[246] M. H. Kim,[238] S. Kim,[247] Y.-M. Kim,[246] C. Kimball,[96] K. Kimes,[54] M. Kinnear,[33] J. S. Kissel,[2] S. Klimenko,[46] A. M. Knee,[114] E. J. Knox,[77] N. Knust,[8,9] K. Kobayashi,[204] S. M. Koehlenbeck,[89] G. Koekoek,[37,36] K. Kohri,[248,249] K. Kokeyama,[33,250] S. Koley,[44,165] P. Kolitsidou,[118] A. E. Koloniari,[251] K. Komori,[42] A. K. H. Kong,[142] A. Kontos,[252] L. M. Koponen,[118] M. Korobko,[97] X. Kou,[18] A. Koushik,[23] N. Kouvatsos,[67] M. Kovalam,[72] T. Koyama,[151] D. B. Kozak,[11] S. L. Kranzhoff,[36,37] V. Kringel,[8,9] N. V. Krishnendu,[118] S. Kroker,[253] A. Królak,[254,186] K. Kruska,[8,9] J. Kubisz,[255] G. Kuehn,[8,9] S. Kulkarni,[216] A. Kulur Ramamohan,[34] Achal Kumar,[46] Anil Kumar,[233] Praveen Kumar,[177] Prayush Kumar,[24] Rahul Kumar,[2] Rakesh Kumar,[93] J. Kume,[256,257,42] K. Kuns,[35] N. Kuntimaddi,[33] S. Kuroyanagi,[208,258] S. Kuwahara,[42] K. Kwak,[239] K. Kwan,[34] S. Kwon,[42] G. Lacaille,[86] D. Laghi,[188,100] A. H. Laity,[163] E. Lalande,[259] M. Lalleman,[23] P. C. Lalremruati,[260] M. Landry,[2] B. B. Lane,[35] R. N. Lang,[35] J. Lange,[120] R. Langgin,[213] B. Lantz,[89] I. La Rosa,[98] J. Larsen,[200] A. Lartaux-Vollard,[41] P. D. Lasky,[6] J. Lawrence,[164] M. Laxen,[63] C. Lazarte,[138] A. Lazzarini,[11] C. Lazzaro,[156,155] P. Leaci,[39,38] L. Leali,[18] Y. K. Lecoeuche,[114] H. M. Lee,[261] H. W. Lee,[262] J. Lee,[78] K. Lee,[238] R.-K. Lee,[142] R. Lee,[35] Sungho Lee,[246] Sunjae Lee,[238] Y. Lee,[141] I. N. Legred,[11] J. Lehmann,[8,9] L. Lehner,[182] M. Le Jean,[175,116] A. Lemaître,[263] M. Lenti,[61,176] M. Leonardi,[74,75,264] M. Lequime,[40] N. Leroy,[41] M. Lesovsky,[11] N. Letendre,[31] M. Lethuillier,[56] Y. Levin,[6] K. Leyde,[73] A. K. Y. Li,[11] K. L. Li,[265] T. G. F. Li,[109] X. Li,[148] Y. Li,[96] Z. Li,[86] A. Lihos,[123] E. T. Lin,[142] F. Lin,[141] L. C.-C. Lin,[265] Y.-C. Lin,[142] C. Lindsay,[201] S. D. Linker,[180] A. Liu,[219] G. C. Liu,[228] Jian Liu,[72] F. Llamas Villarreal,[164] J. Llobera-Querol,[98] R. K. L. Lo,[140] J.-P. Locquet,[109] S. C. G. Loggins,[266] M. R. Loizou,[133] L. T. London,[67] A. Longo,[60,61] D. Lopez,[165] M. Lopez Portilla,[71] M. Lorenzini,[21,22] A. Lorenzo-Medina,[177] V. Loriette,[41] M. Lormand,[63] G. Losurdo,[267,80] E. Lotti,[133] T. P. Lott IV,[57] J. D. Lough,[8,9] H. A. Loughlin,[35] C. O. Lousto,[110] N. Low,[124] N. Lu,[34] L. Lucchesi,[80] H. Lück,[9,8,9] D. Lumaca,[22] A. P. Lundgren,[268,269] A. W. Lussier,[259] R. Macas,[73] M. MacInnis,[35] D. M. Macleod,[33] I. A. O. MacMillan,[11] A. Macquet,[41] K. Maeda,[151] S. Maenaut,[109] S. S. Magare,[79] R. M. Magee,[11] E. Maggio,[1] R. Maggiore,[37,107] M. Magnozzi,[29,30] M. Mahesh,[97] M. Maini,[163] S. Majhi,[79] E. Majorana,[39,38] C. N. Makarem,[11] D. Malakar,[105] J. A. Malaquias-Reis,[19] U. Mali,[190] S. Maliakal,[11] A. Malik,[103] L. Mallick,[168,190] A.-K. Malz,[58] N. Man,[113] M. Mancarella,[99] V. Mandic,[18] V. Mangano,[170,155] B. Mannix,[77] G. L. Mansell,[78] M. Manske,[10] M. Mantovani,[62] M. Mapelli,[91,92,270] C. Marinelli,[101] F. Marion,[31] A. S. Markosyan,[89] A. Markowitz,[11] E. Maros,[11] S. Marsat,[100] F. Martelli,[60,61] I. W. Martin,[86] R. M. Martin,[193] B. B. Martinez,[131] D. A. Martinez,[54] M. Martinez,[43,271] V. Martinez,[129] A. Martini,[74,75] J. C. Martins,[19] D. V. Martynov,[118] E. J. Marx,[35] L. Massaro,[36,37] A. Masserot,[31] M. Masso-Reid,[86] S. Mastrogiovanni,[38] T. Matcovich,[51] M. Matiushechkina,[8,9] N. Mavalvala,[35] N. Maxwell,[2] G. McCarrol,[63] R. McCarthy,[2] D. E. McClelland,[34] S. McCormick,[63] L. McCuller,[11] S. McEachin,[123] C. McElhenny,[123] G. I. McGhee,[86] J. McGinn,[86] K. B. M. McGowan,[144] J. McIver,[114]

A. McLeod,[72] I. McMahon,[188] T. McRae,[34] R. McTeague,[86] D. Meacher,[10] B. N. Meagher,[78] R. Mechum,[110] Q. Meijer,[71] A. Melatos,[124] C. S. Menoni,[137] F. Mera,[2] R. A. Mercer,[10] L. Mereni,[175] K. Merfeld,[162] E. L. Merilh,[63] J. R. Mérou,[98] J. D. Merritt,[77] M. Merzougui,[113] C. Messick,[10] B. Mestichelli,[44] M. Meyer-Conde,[272] P. M. Meyers,[11] F. Meylahn,[8,9] A. Mhaske,[79] A. Miani,[74,75] H. Miao,[273] C. Michel,[175] Y. Michimura,[42] H. Middleton,[118] D. P. Mihaylov,[104] S. J. Miller,[11] M. Millhouse,[57] E. Milotti,[184,48] V. Milotti,[91] Y. Minenkov,[22] E. M. Minihan,[65] Ll. M. Mir,[43] L. Mirasola,[155,156] M. Miravet-Tenés,[138] C.-A. Miritescu,[43] A. Mishra,[24] C. Mishra,[106] T. Mishra,[46] A. L. Mitchell,[37,107] J. G. Mitchell,[65] S. Mitra,[79] V. P. Mitrofanov,[108] K. Mitsuhashi,[25] R. Mittleman,[35] O. Miyakawa,[50] S. Miyoki,[50] A. Miyoko,[65] G. Mo,[35] L. Mobilia,[60,61] S. R. P. Mohapatra,[11] S. R. Mohite,[7] M. Molina-Ruiz,[207] M. Mondin,[180] J. K. Monsalve,[189] M. Montani,[60,61] C. J. Moore,[224] D. Moraru,[2] A. More,[79] S. More,[79] C. Moreno,[135] E. A. Moreno,[35] G. Moreno,[2] A. Moreso Serra,[82] S. Morisaki,[42,204] Y. Moriwaki,[151] G. Morras,[208] A. Moscatello,[91] M. Mould,[35] B. Mours,[64] C. M. Mow-Lowry,[37,107] L. Muccillo,[176,61] F. Muciaccia,[39,38] D. Mukherjee,[118] Samanwaya Mukherjee,[24] Soma Mukherjee,[164] Subroto Mukherjee,[93] Suvodip Mukherjee,[13] N. Mukund,[35] A. Mullavey,[63] H. Mullock,[114] J. Mundi,[220] C. L. Mungioli,[72] M. Murakoshi,[230] P. G. Murray,[86] D. Nabari,[74,75] S. L. Nadji,[8,9] A. Nagar,[28,274] N. Nagarajan,[86] K. Nakagaki,[50] K. Nakamura,[25] H. Nakano,[275] M. Nakano,[11] D. Nanadoumgar-Lacroze,[43] D. Nandi,[12] V. Napolano,[62] P. Narayan,[216] I. Nardecchia,[22] T. Narikawa,[204] H. Narola,[71] L. Naticchioni,[38] R. K. Nayak,[260] L. Negri,[71] A. Nela,[86] C. Nelle,[77] A. Nelson,[131] T. J. N. Nelson,[63] M. Nery,[8,9] A. Neunzert,[2] S. Ng,[54] L. Nguyen Quynh,[276] S. A. Nichols,[12] A. B. Nielsen,[277] Y. Nishino,[25,42] A. Nishizawa,[278] S. Nissanke,[279,37] W. Niu,[7] F. Nocera,[62] J. Noller,[280] M. Norman,[33] C. North,[33] J. Novak,[116,234,281] R. Nowicki,[144] J. F. Nuño Siles,[208] L. K. Nuttall,[73] K. Obayashi,[230] J. Oberling,[2] J. O'Dell,[229] E. Oelker,[35] M. Oertel,[234,116,282,281] G. Oganesyan,[44,45] T. O'Hanlon,[63] M. Ohashi,[50] F. Ohme,[8,9] R. Oliveri,[116,282,281] R. Omer,[18] B. O'Neal,[123] M. Onishi,[151] K. Oohara,[283] B. O'Reilly,[63] M. Orselli,[51,76] R. O'Shaughnessy,[110] S. O'Shea,[86] S. Oshino,[50] C. Osthelder,[11] I. Ota,[12] D. J. Ottaway,[115] A. Ouzriat,[56] H. Overmier,[63] B. J. Owen,[284] R. Ozaki,[230] A. E. Pace,[7] R. Pagano,[12] M. A. Page,[25] A. Pai,[195] L. Paiella,[44] A. Pal,[285] S. Pal,[260] M. A. Palaia,[80,81] M. Pálfi,[203] P. P. Palma,[39,21,22] C. Palomba,[38] P. Palud,[20] H. Pan,[142] J. Pan,[72] K. C. Pan,[142] P. K. Panda,[233] Shiksha Pandey,[7] Swadha Pandey,[35] P. T. H. Pang,[37,71] F. Pannarale,[39,38] K. A. Pannone,[54] B. C. Pant,[103] F. H. Panther,[72] M. Panzeri,[60,61] F. Paoletti,[80] A. Paolone,[38,286] A. Papadopoulos,[86] E. E. Papalexakis,[211] L. Papalini,[80,81] G. Papigkiotis,[251] A. Paquis,[41] A. Parisi,[76,51] B.-J. Park,[246] J. Park,[287] W. Parker,[63] G. Pascale,[8,9] D. Pascucci,[94] A. Pasqualetti,[62] R. Passaquieti,[81,80] L. Passenger,[6] D. Passuello,[80] O. Patane,[2] A. V. Patel,[141] D. Pathak,[79] A. Patra,[33] B. Patricelli,[81,80] B. G. Patterson,[33] K. Paul,[106] S. Paul,[77] E. Payne,[11] T. Pearce,[33] M. Pedraza,[11] A. Pele,[11] F. E. Peña Arellano,[288] X. Peng,[118] Y. Peng,[57] S. Penn,[289] M. D. Penuliar,[54] A. Perego,[74,75] Z. Pereira,[133] C. Périgois,[290,92,91] G. Perna,[91] A. Perreca,[74,75,44] J. Perret,[20] S. Perriès,[56] J. W. Perry,[37,107] D. Pesios,[251] S. Peters,[165] S. Petracca,[206] C. Petrillo,[76] H. P. Pfeiffer,[1] H. Pham,[63] K. A. Pham,[18] K. S. Phukon,[118] H. Phurailatpam,[219] M. Piarulli,[100] L. Piccari,[39,38] O. J. Piccinni,[34] M. Pichot,[113] M. Piendibene,[81,80] F. Piergiovanni,[60,61] L. Pierini,[38] G. Pierra,[38] V. Pierro,[291,132] M. Pietrzak,[95] M. Pillas,[165] F. Pilo,[80] L. Pinard,[175] I. M. Pinto,[291,132,292,32] M. Pinto,[62] B. J. Piotrzkowski,[10] M. Pirello,[2] M. D. Pitkin,[224,86] A. Placidi,[51] E. Placidi,[39,38] M. L. Planas,[98] W. Plastino,[212,22] C. Plunkett,[35] R. Poggiani,[81,80] E. Polini,[35] J. Pomper,[80,81] L. Pompili,[1] J. Poon,[219] E. Porcelli,[37] E. K. Porter,[20] C. Posnansky,[7] R. Poulton,[62] J. Powell,[154] G. S. Prabhu,[79] M. Pracchia,[165] B. K. Pradhan,[79] T. Pradier,[64] A. K. Prajapati,[93] K. Prasai,[293] R. Prasanna,[233] P. Prasia,[79] G. Pratten,[118] G. Principe,[184,48] G. A. Prodi,[74,75] P. Prosperi,[80] P. Prosposito,[21,22] A. C. Providence,[65] A. Puecher,[1] J. Pullin,[12] P. Puppo,[38] M. Pürrer,[163] H. Qi,[16] J. Qin,[34] G. Quéméner,[173,116] V. Quetschke,[164] L. H. Quiceno,[189] P. J. Quinonez,[65] N. Qutob,[57] R. Rading,[231] I. Rainho,[138] S. Raja,[103] C. Rajan,[103] B. Rajbhandari,[110] K. E. Ramirez,[63] F. A. Ramis Vidal,[98] M. Ramos Arevalo,[164] A. Ramos-Buades,[98,37] S. Ranjan,[57] K. Ransom,[63] P. Rapagnani,[39,38] B. Ratto,[65] A. Ravichandran,[133] A. Ray,[96] V. Raymond,[33] M. Razzano,[81,80] J. Read,[54] T. Regimbau,[31] S. Reid,[55] C. Reissel,[35] D. H. Reitze,[11] A. I. Renzini,[11] A. Renzini,[127] B. Revenu,[294,41] A. Revilla Peña,[82] R. Reyes,[180] L. Ricca,[15] F. Ricci,[39,38] M. Ricci,[38,39] A. Ricciardone,[81,80] J. Rice,[78] J. W. Richardson,[211] M. L. Richardson,[115] A. Rijal,[65] K. Riles,[90] H. K. Riley,[33] S. Rinaldi,[270] J. Rittmeyer,[97] C. Robertson,[229] F. Robinet,[41] M. Robinson,[2] A. Rocchi,[22] L. Rolland,[31] J. G. Rollins,[11] A. E. Romano,[189] J. D. Romano,[164] R. Romano,[3,4] A. Romero,[31] I. M. Romero-Shaw,[224] J. H. Romie,[63] S. Ronchini,[7] T. J. Roocke,[115] L. Rosa,[4,32] T. J. Rosauer,[211] C. A. Rose,[57] D. Rosińska,[125] M. P. Ross,[53]

M. Rossello-Sastre,[98] S. Rowan,[86] S. K. Roy,[191,192] S. Roy,[15] D. Rozza,[127,128] P. Ruggi,[62] N. Ruhama,[239] E. Ruiz Morales,[295,208] K. Ruiz-Rocha,[144] S. Sachdev,[57] T. Sadecki,[2] P. Saffarieh,[37,107] S. Safi-Harb,[168] M. R. Sah,[13] S. Saha,[142] T. Sainrat,[64] S. Sajith Menon,[215,39,38] K. Sakai,[296] Y. Sakai,[272] M. Sakellariadou,[67] S. Sakon,[7] O. S. Salafia,[158,128,127] F. Salces-Carcoba,[11] L. Salconi,[62] M. Saleem,[120] F. Salemi,[39,38] M. Sallé,[37] S. U. Salunkhe,[79] S. Salvador,[173,172] A. Salvarese,[120] A. Samajdar,[71,37] A. Sanchez,[2] E. J. Sanchez,[11] L. E. Sanchez,[11] N. Sanchis-Gual,[138] J. R. Sanders,[181] E. M. Sänger,[1] F. Santoliquido,[44,45] F. Sarandrea,[28] T. R. Saravanan,[79] N. Sarin,[6] P. Sarkar,[8,9] A. Sasli,[251] P. Sassi,[51,76] B. Sassolas,[175] B. S. Sathyaprakash,[7,33] R. Sato,[227] S. Sato,[151] Yukino Sato,[151] Yu Sato,[151] O. Sauter,[46] R. L. Savage,[2] T. Sawada,[50] H. L. Sawant,[79] S. Sayah,[175] V. Scacco,[21,22] D. Schaetzl,[11] M. Scheel,[148] A. Schiebelbein,[190] M. G. Schiworski,[78] P. Schmidt,[118] S. Schmidt,[71] R. Schnabel,[97] M. Schneewind,[8,9] R. M. S. Schofield,[77] K. Schouteden,[109] B. W. Schulte,[8,9] B. F. Schutz,[33,8,9] E. Schwartz,[297] M. Scialpi,[298] J. Scott,[86] S. M. Scott,[34] R. M. Sedas,[63] T. C. Seetharamu,[86] M. Seglar-Arroyo,[43] Y. Sekiguchi,[299] D. Sellers,[63] N. Sembo,[205] A. S. Sengupta,[300] E. G. Seo,[86] J. W. Seo,[109] V. Sequino,[32,4] M. Serra,[38] A. Sevrin,[187] T. Shaffer,[2] U. S. Shah,[57] M. A. Shaikh,[261] L. Shao,[301] A. K. Sharma,[98] Preeti Sharma,[12] Prianka Sharma,[103] Ritwik Sharma,[18] S. Sharma Chaudhary,[105] P. Shawhan,[126] N. S. Shcheblanov,[302,263] E. Sheridan,[144] Z.-H. Shi,[142] M. Shikauchi,[42] R. Shimomura,[303] H. Shinkai,[303] S. Shirke,[79] D. H. Shoemaker,[35] D. M. Shoemaker,[120] R. W. Short,[2] S. ShyamSundar,[103] A. Sider,[157] H. Siegel,[191,192] D. Sigg,[2] L. Silenzi,[36,37] L. Silvestri,[39,169] M. Simmonds,[115] L. P. Singer,[304] Amitesh Singh,[216] Anika Singh,[11] D. Singh,[207] N. Singh,[98] S. Singh,[217,59] A. M. Sintes,[98] V. Sipala,[170,155] V. Skliris,[33] B. J. J. Slagmolen,[34] D. A. Slater,[200] T. J. Slaven-Blair,[72] J. Smetana,[118] J. R. Smith,[54] L. Smith,[86,184,48] R. J. E. Smith,[6] W. J. Smith,[144] S. Soares de Albuquerque Filho,[60] M. Soares-Santos,[188] K. Somiya,[217] I. Song,[142] S. Soni,[35] V. Sordini,[56] F. Sorrentino,[29] H. Sotani,[305] F. Spada,[80] V. Spagnuolo,[37] A. P. Spencer,[86] P. Spinicelli,[62] A. K. Srivastava,[93] F. Stachurski,[86] C. J. Stark,[123] D. A. Steer,[306] N. Steinle,[168] J. Steinlechner,[36,37] S. Steinlechner,[36,37] N. Stergioulas,[251] P. Stevens,[41] M. StPierre,[163] M. D. Strong,[12] A. Strunk,[2] A. L. Stuver,[102,*] M. Suchenek,[95] S. Sudhagar,[95] Y. Sudo,[230] N. Sueltmann,[97] L. Suleiman,[54] K. D. Sullivan,[12] J. Sun,[241] L. Sun,[34] S. Sunil,[93] J. Suresh,[113] B. J. Sutton,[67] P. J. Sutton,[33] K. Suzuki,[217] M. Suzuki,[204] B. L. Swinkels,[37] A. Syx,[116] M. J. Szczepańczyk,[307] P. Szewczyk,[125] M. Tacca,[37] H. Tagoshi,[204] K. Takada,[204] H. Takahashi,[272] R. Takahashi,[25] A. Takamori,[42] S. Takano,[308] H. Takeda,[309,310] K. Takeshita,[217] I. Takimoto Schmiegelow,[44,45] M. Takou-Ayaoh,[78] C. Talbot,[130] M. Tamaki,[204] N. Tamanini,[100] D. Tanabe,[141] K. Tanaka,[50] S. J. Tanaka,[230] S. Tanioka,[33] D. B. Tanner,[46] W. Tanner,[8,9] L. Tao,[211] R. D. Tapia,[7] E. N. Tapia San Martín,[37] C. Taranto,[21,22] A. Taruya,[311] J. D. Tasson,[152] J. G. Tau,[110] D. Tellez,[54] R. Tenorio,[98] H. Themann,[180] A. Theodoropoulos,[138] M. P. Thirugnanasambandam,[79] L. M. Thomas,[11] M. Thomas,[63] P. Thomas,[2] J. E. Thompson,[210] S. R. Thondapu,[103] K. A. Thorne,[63] E. Thrane,[6] J. Tissino,[44,45] A. Tiwari,[79] Pawan Tiwari,[44] Praveer Tiwari,[195] S. Tiwari,[188] V. Tiwari,[118] M. R. Todd,[78] M. Toffano,[91] A. M. Toivonen,[18] K. Toland,[86] A. E. Tolley,[73] T. Tomaru,[25] V. Tommasini,[11] T. Tomura,[50] H. Tong,[6] C. Tong-Yu,[141] A. Torres-Forné,[138,139] C. I. Torrie,[11] I. Tosta e Melo,[312] E. Tournefier,[31] M. Trad Nery,[113] K. Tran,[123] A. Trapananti,[52,51] R. Travaglini,[167] F. Travasso,[52,51] G. Traylor,[63] M. Trevor,[126] M. C. Tringali,[62] A. Tripathee,[90] G. Troian,[184,48] A. Trovato,[184,48] L. Trozzo,[4] R. J. Trudeau,[11] T. Tsang,[33] S. Tsuchida,[313] L. Tsukada,[213] K. Turbang,[187,23] M. Turconi,[113] C. Turski,[94] H. Ubach,[82,83] N. Uchikata,[204] T. Uchiyama,[50] R. P. Udall,[11] T. Uehara,[314] K. Ueno,[42] V. Undheim,[277] L. E. Uronen,[219] T. Ushiba,[50] M. Vacatello,[80,81] H. Vahlbruch,[8,9] N. Vaidya,[11] G. Vajente,[11] A. Vajpeyi,[6] J. Valencia,[98] M. Valentini,[107,37] S. A. Vallejo-Peña,[189] S. Vallero,[28] V. Valsan,[10] M. van Dael,[37,315] E. Van den Bossche,[187] J. F. J. van den Brand,[36,107,37] C. Van Den Broeck,[71,37] M. van der Sluys,[37,71] A. Van de Walle,[41] J. van Dongen,[37,107] K. Vandra,[102] M. VanDyke,[119] H. van Haevermaet,[23] J. V. van Heijningen,[37,107] P. Van Hove,[64] J. Vanier,[259] M. VanKeuren,[104] J. Vanosky,[2] N. van Remortel,[23] M. Vardaro,[36,37] A. F. Vargas,[124] V. Varma,[133] A. N. Vazquez,[89] A. Vecchio,[118] G. Vedovato,[92] J. Veitch,[86] P. J. Veitch,[115] S. Venikoudis,[15] R. C. Venterea,[18] P. Verdier,[56] M. Vereecken,[15] D. Verkindt,[31] B. Verma,[133] Y. Verma,[103] S. M. Vermeulen,[11] F. Vetrano,[60] A. Veutro,[38,39] A. Viceré,[60,61] S. Vidyant,[78] A. D. Viets,[88] A. Vijaykumar,[190] A. Vilkha,[110] N. Villanueva Espinosa,[138] V. Villa-Ortega,[177] E. T. Vincent,[57] J.-Y. Vinet,[113] S. Viret,[56] S. Vitale,[35] H. Vocca,[76,51] D. Voigt,[97] E. R. G. von Reis,[2] J. S. A. von Wrangel,[8,9] W. E. Vossius,[231] L. Vujeva,[140] S. P. Vyatchanin,[108] J. Wack,[11] L. E. Wade,[104] M. Wade,[104] K. J. Wagner,[110] L. Wallace,[11] E. J. Wang,[89] H. Wang,[217] J. Z. Wang,[90] W. H. Wang,[164] Y. F. Wang,[1] G. Waratkar,[195] J. Warner,[2] M. Was,[31] T. Washimi,[25] N. Y. Washington,[11] D. Watarai,[42]

B. Weaver,[2] S. A. Webster,[86] N. L. Weickhardt,[97] M. Weinert,[8, 9] A. J. Weinstein,[11] R. Weiss,[35] L. Wen,[72] K. Wette,[34] J. T. Whelan,[110] B. F. Whiting,[46] C. Whittle,[11] E. G. Wickens,[73] D. Wilken,[8, 9, 9] A. T. Wilkin,[211] B. M. Williams,[119] D. Williams,[86] M. J. Williams,[73] N. S. Williams,[1] J. L. Willis,[11] B. Willke,[9, 8, 9] M. Wils,[109] L. Wilson,[104] C. W. Winborn,[105] J. Winterflood,[72] C. C. Wipf,[11] G. Woan,[86] J. Woehler,[36, 37] N. E. Wolfe,[35] H. T. Wong,[141] I. C. F. Wong,[219, 109] K. Wong,[190] T. Wouters,[71, 37] J. L. Wright,[2] M. Wright,[86, 71] B. Wu,[78] C. Wu,[142] D. S. Wu,[8, 9] H. Wu,[142] K. Wu,[119] Q. Wu,[53] T. Y. Wu,[316, 317] Y. Wu,[96] Z. Wu,[100] E. Wuchner,[54] D. M. Wysocki,[10] V. A. Xu,[207] Y. Xu,[98] N. Yadav,[28] H. Yamamoto,[11] K. Yamamoto,[151] T. S. Yamamoto,[42] T. Yamamoto,[50] R. Yamazaki,[230] T. Yan,[118] K. Z. Yang,[18] Y. Yang,[146] Z. Yarbrough,[12] J. Yebana,[98] S.-W. Yeh,[142] A. B. Yelikar,[144] X. Yin,[35] J. Yokoyama,[318, 42] T. Yokozawa,[50] S. Yuan,[72] H. Yuzurihara,[50] M. Zanolin,[65] M. Zeeshan,[110] T. Zelenova,[62] J.-P. Zendri,[92] M. Zeoli,[15] M. Zerrad,[40] M. Zevin,[96] L. Zhang,[11] N. Zhang,[57] R. Zhang,[149] T. Zhang,[118] C. Zhao,[72] Yue Zhao,[161] Yuhang Zhao,[20] Z.-C. Zhao,[319] Y. Zheng,[105] H. Zhong,[18] H. Zhou,[78] H. O. Zhu,[72] Z.-H. Zhu,[319, 320] A. B. Zimmerman,[120] L. Zimmermann,[56] M. E. Zucker,[35, 11] and J. Zweizig[11]

(The LIGO Scientific Collaboration, the Virgo Collaboration, and the KAGRA Collaboration)

[1] *Max Planck Institute for Gravitational Physics (Albert Einstein Institute), D-14476 Potsdam, Germany*
[2] *LIGO Hanford Observatory, Richland, WA 99352, USA*
[3] *Dipartimento di Farmacia, Università di Salerno, I-84084 Fisciano, Salerno, Italy*
[4] *INFN, Sezione di Napoli, I-80126 Napoli, Italy*
[5] *University of Warwick, Coventry CV4 7AL, United Kingdom*
[6] *OzGrav, School of Physics & Astronomy, Monash University, Clayton 3800, Victoria, Australia*
[7] *The Pennsylvania State University, University Park, PA 16802, USA*
[8] *Max Planck Institute for Gravitational Physics (Albert Einstein Institute), D-30167 Hannover, Germany*
[9] *Leibniz Universität Hannover, D-30167 Hannover, Germany*
[10] *University of Wisconsin-Milwaukee, Milwaukee, WI 53201, USA*
[11] *LIGO Laboratory, California Institute of Technology, Pasadena, CA 91125, USA*
[12] *Louisiana State University, Baton Rouge, LA 70803, USA*
[13] *Tata Institute of Fundamental Research, Mumbai 400005, India*
[14] *Centre de Physique Théorique, Aix-Marseille Université, Campus de Luminy, 163 Av. de Luminy, 13009 Marseille, France*
[15] *Université catholique de Louvain, B-1348 Louvain-la-Neuve, Belgium*
[16] *Queen Mary University of London, London E1 4NS, United Kingdom*
[17] *University of California, Davis, Davis, CA 95616, USA*
[18] *University of Minnesota, Minneapolis, MN 55455, USA*
[19] *Instituto Nacional de Pesquisas Espaciais, 12227-010 São José dos Campos, São Paulo, Brazil*
[20] *Université Paris Cité, CNRS, Astroparticule et Cosmologie, F-75013 Paris, France*
[21] *Università di Roma Tor Vergata, I-00133 Roma, Italy*
[22] *INFN, Sezione di Roma Tor Vergata, I-00133 Roma, Italy*
[23] *Universiteit Antwerpen, 2000 Antwerpen, Belgium*
[24] *International Centre for Theoretical Sciences, Tata Institute of Fundamental Research, Bengaluru 560089, India*
[25] *Gravitational Wave Science Project, National Astronomical Observatory of Japan, 2-21-1 Osawa, Mitaka City, Tokyo 181-8588, Japan*
[26] *Advanced Technology Center, National Astronomical Observatory of Japan, 2-21-1 Osawa, Mitaka City, Tokyo 181-8588, Japan*
[27] *Theoretisch-Physikalisches Institut, Friedrich-Schiller-Universität Jena, D-07743 Jena, Germany*
[28] *INFN Sezione di Torino, I-10125 Torino, Italy*
[29] *INFN, Sezione di Genova, I-16146 Genova, Italy*
[30] *Dipartimento di Fisica, Università degli Studi di Genova, I-16146 Genova, Italy*
[31] *Univ. Savoie Mont Blanc, CNRS, Laboratoire d'Annecy de Physique des Particules - IN2P3, F-74000 Annecy, France*
[32] *Università di Napoli "Federico II", I-80126 Napoli, Italy*
[33] *Cardiff University, Cardiff CF24 3AA, United Kingdom*
[34] *OzGrav, Australian National University, Canberra, Australian Capital Territory 0200, Australia*
[35] *LIGO Laboratory, Massachusetts Institute of Technology, Cambridge, MA 02139, USA*
[36] *Maastricht University, 6200 MD Maastricht, Netherlands*
[37] *Nikhef, 1098 XG Amsterdam, Netherlands*
[38] *INFN, Sezione di Roma, I-00185 Roma, Italy*
[39] *Università di Roma "La Sapienza", I-00185 Roma, Italy*
[40] *Aix Marseille Univ, CNRS, Centrale Med, Institut Fresnel, F-13013 Marseille, France*
[41] *Université Paris-Saclay, CNRS/IN2P3, IJCLab, 91405 Orsay, France*
[42] *University of Tokyo, Tokyo, 113-0033, Japan*
[43] *Institut de Física d'Altes Energies (IFAE), The Barcelona Institute of Science and Technology, Campus UAB, E-08193 Bellaterra (Barcelona), Spain*

[44] Gran Sasso Science Institute (GSSI), I-67100 L'Aquila, Italy
[45] INFN, Laboratori Nazionali del Gran Sasso, I-67100 Assergi, Italy
[46] University of Florida, Gainesville, FL 32611, USA
[47] Dipartimento di Scienze Matematiche, Informatiche e Fisiche, Università di Udine, I-33100 Udine, Italy
[48] INFN, Sezione di Trieste, I-34127 Trieste, Italy
[49] Tecnologico de Monterrey, Escuela de Ingeniería y Ciencias, 64849 Monterrey, Nuevo León, Mexico
[50] Institute for Cosmic Ray Research, KAGRA Observatory, The University of Tokyo, 238 Higashi-Mozumi, Kamioka-cho, Hida City, Gifu 506-1205, Japan
[51] INFN, Sezione di Perugia, I-06123 Perugia, Italy
[52] Università di Camerino, I-62032 Camerino, Italy
[53] University of Washington, Seattle, WA 98195, USA
[54] California State University Fullerton, Fullerton, CA 92831, USA
[55] SUPA, University of Strathclyde, Glasgow G1 1XQ, United Kingdom
[56] Université Claude Bernard Lyon 1, CNRS, IP2I Lyon / IN2P3, UMR 5822, F-69622 Villeurbanne, France
[57] Georgia Institute of Technology, Atlanta, GA 30332, USA
[58] Royal Holloway, University of London, London TW20 0EX, United Kingdom
[59] Astronomical course, The Graduate University for Advanced Studies (SOKENDAI), 2-21-1 Osawa, Mitaka City, Tokyo 181-8588, Japan
[60] Università degli Studi di Urbino "Carlo Bo", I-61029 Urbino, Italy
[61] INFN, Sezione di Firenze, I-50019 Sesto Fiorentino, Firenze, Italy
[62] European Gravitational Observatory (EGO), I-56021 Cascina, Pisa, Italy
[63] LIGO Livingston Observatory, Livingston, LA 70754, USA
[64] Université de Strasbourg, CNRS, IPHC UMR 7178, F-67000 Strasbourg, France
[65] Embry-Riddle Aeronautical University, Prescott, AZ 86301, USA
[66] Dipartimento di Fisica "E.R. Caianiello", Università di Salerno, I-84084 Fisciano, Salerno, Italy
[67] King's College London, University of London, London WC2R 2LS, United Kingdom
[68] Korea Institute of Science and Technology Information, Daejeon 34141, Republic of Korea
[69] International College, Osaka University, 1-1 Machikaneyama-cho, Toyonaka City, Osaka 560-0043, Japan
[70] Accelerator Laboratory, High Energy Accelerator Research Organization (KEK), 1-1 Oho, Tsukuba City, Ibaraki 305-0801, Japan
[71] Institute for Gravitational and Subatomic Physics (GRASP), Utrecht University, 3584 CC Utrecht, Netherlands
[72] OzGrav, University of Western Australia, Crawley, Western Australia 6009, Australia
[73] University of Portsmouth, Portsmouth, PO1 3FX, United Kingdom
[74] Università di Trento, Dipartimento di Fisica, I-38123 Povo, Trento, Italy
[75] INFN, Trento Institute for Fundamental Physics and Applications, I-38123 Povo, Trento, Italy
[76] Università di Perugia, I-06123 Perugia, Italy
[77] University of Oregon, Eugene, OR 97403, USA
[78] Syracuse University, Syracuse, NY 13244, USA
[79] Inter-University Centre for Astronomy and Astrophysics, Pune 411007, India
[80] INFN, Sezione di Pisa, I-56127 Pisa, Italy
[81] Università di Pisa, I-56127 Pisa, Italy
[82] Institut de Ciències del Cosmos (ICCUB), Universitat de Barcelona (UB), c. Martí i Franquès, 1, 08028 Barcelona, Spain
[83] Departament de Física Quàntica i Astrofísica (FQA), Universitat de Barcelona (UB), c. Martí i Franqués, 1, 08028 Barcelona, Spain
[84] Institut d'Estudis Espacials de Catalunya, c. Gran Capità, 2-4, 08034 Barcelona, Spain
[85] Dipartimento di Medicina, Chirurgia e Odontoiatria "Scuola Medica Salernitana", Università di Salerno, I-84081 Baronissi, Salerno, Italy
[86] IGR, University of Glasgow, Glasgow G12 8QQ, United Kingdom
[87] HUN-REN Wigner Research Centre for Physics, H-1121 Budapest, Hungary
[88] Concordia University Wisconsin, Mequon, WI 53097, USA
[89] Stanford University, Stanford, CA 94305, USA
[90] University of Michigan, Ann Arbor, MI 48109, USA
[91] Università di Padova, Dipartimento di Fisica e Astronomia, I-35131 Padova, Italy
[92] INFN, Sezione di Padova, I-35131 Padova, Italy
[93] Institute for Plasma Research, Bhat, Gandhinagar 382428, India
[94] Universiteit Gent, B-9000 Gent, Belgium
[95] Nicolaus Copernicus Astronomical Center, Polish Academy of Sciences, 00-716, Warsaw, Poland
[96] Northwestern University, Evanston, IL 60208, USA
[97] Universität Hamburg, D-22761 Hamburg, Germany
[98] IAC3–IEEC, Universitat de les Illes Balears, E-07122 Palma de Mallorca, Spain
[99] Aix-Marseille Université, Université de Toulon, CNRS, CPT, Marseille, France
[100] Laboratoire des 2 Infinis - Toulouse (L2IT-IN2P3), F-31062 Toulouse Cedex 9, France

[101] *Università di Siena, Dipartimento di Scienze Fisiche, della Terra e dell'Ambiente, I-53100 Siena, Italy*
[102] *Villanova University, Villanova, PA 19085, USA*
[103] *RRCAT, Indore, Madhya Pradesh 452013, India*
[104] *Kenyon College, Gambier, OH 43022, USA*
[105] *Missouri University of Science and Technology, Rolla, MO 65409, USA*
[106] *Indian Institute of Technology Madras, Chennai 600036, India*
[107] *Department of Physics and Astronomy, Vrije Universiteit Amsterdam, 1081 HV Amsterdam, Netherlands*
[108] *Lomonosov Moscow State University, Moscow 119991, Russia*
[109] *Katholieke Universiteit Leuven, Oude Markt 13, 3000 Leuven, Belgium*
[110] *Rochester Institute of Technology, Rochester, NY 14623, USA*
[111] *Université libre de Bruxelles, 1050 Bruxelles, Belgium*
[112] *Bar-Ilan University, Ramat Gan, 5290002, Israel*
[113] *Université Côte d'Azur, Observatoire de la Côte d'Azur, CNRS, Artemis, F-06304 Nice, France*
[114] *University of British Columbia, Vancouver, BC V6T 1Z4, Canada*
[115] *OzGrav, University of Adelaide, Adelaide, South Australia 5005, Australia*
[116] *Centre national de la recherche scientifique, 75016 Paris, France*
[117] *Univ Rennes, CNRS, Institut FOTON - UMR 6082, F-35000 Rennes, France*
[118] *University of Birmingham, Birmingham B15 2TT, United Kingdom*
[119] *Washington State University, Pullman, WA 99164, USA*
[120] *University of Texas, Austin, TX 78712, USA*
[121] *Cornell University, Ithaca, NY 14850, USA*
[122] *Laboratoire Kastler Brossel, Sorbonne Université, CNRS, ENS-Université PSL, Collège de France, F-75005 Paris, France*
[123] *Christopher Newport University, Newport News, VA 23606, USA*
[124] *OzGrav, University of Melbourne, Parkville, Victoria 3010, Australia*
[125] *Astronomical Observatory Warsaw University, 00-478 Warsaw, Poland*
[126] *University of Maryland, College Park, MD 20742, USA*
[127] *Università degli Studi di Milano-Bicocca, I-20126 Milano, Italy*
[128] *INFN, Sezione di Milano-Bicocca, I-20126 Milano, Italy*
[129] *Université de Lyon, Université Claude Bernard Lyon 1, CNRS, Institut Lumière Matière, F-69622 Villeurbanne, France*
[130] *University of Chicago, Chicago, IL 60637, USA*
[131] *University of Arizona, Tucson, AZ 85721, USA*
[132] *INFN, Sezione di Napoli, Gruppo Collegato di Salerno, I-80126 Napoli, Italy*
[133] *University of Massachusetts Dartmouth, North Dartmouth, MA 02747, USA*
[134] *Niels Bohr Institute, Copenhagen University, 2100 København, Denmark*
[135] *Universidad de Guadalajara, 44430 Guadalajara, Jalisco, Mexico*
[136] *Istituto di Astrofisica e Planetologia Spaziali di Roma, 00133 Roma, Italy*
[137] *Colorado State University, Fort Collins, CO 80523, USA*
[138] *Departamento de Astronomía y Astrofísica, Universitat de València, E-46100 Burjassot, València, Spain*
[139] *Observatori Astronòmic, Universitat de València, E-46980 Paterna, València, Spain*
[140] *Niels Bohr Institute, University of Copenhagen, 2100 Kóbenhavn, Denmark*
[141] *National Central University, Taoyuan City 320317, Taiwan*
[142] *National Tsing Hua University, Hsinchu City 30013, Taiwan*
[143] *OzGrav, Charles Sturt University, Wagga Wagga, New South Wales 2678, Australia*
[144] *Vanderbilt University, Nashville, TN 37235, USA*
[145] *University of the Chinese Academy of Sciences / International Centre for Theoretical Physics Asia-Pacific, Bejing 100049, China*
[146] *Department of Electrophysics, National Yang Ming Chiao Tung University, 101 Univ. Street, Hsinchu, Taiwan*
[147] *Kamioka Branch, National Astronomical Observatory of Japan, 238 Higashi-Mozumi, Kamioka-cho, Hida City, Gifu 506-1205, Japan*
[148] *CaRT, California Institute of Technology, Pasadena, CA 91125, USA*
[149] *Northeastern University, Boston, MA 02115, USA*
[150] *Dipartimento di Ingegneria Industriale (DIIN), Università di Salerno, I-84084 Fisciano, Salerno, Italy*
[151] *Faculty of Science, University of Toyama, 3190 Gofuku, Toyama City, Toyama 930-8555, Japan*
[152] *Carleton College, Northfield, MN 55057, USA*
[153] *University of Szeged, Dóm tér 9, Szeged 6720, Hungary*
[154] *OzGrav, Swinburne University of Technology, Hawthorn VIC 3122, Australia*
[155] *INFN Cagliari, Physics Department, Università degli Studi di Cagliari, Cagliari 09042, Italy*
[156] *Università degli Studi di Cagliari, Via Università 40, 09124 Cagliari, Italy*
[157] *Université Libre de Bruxelles, Brussels 1050, Belgium*
[158] *INAF, Osservatorio Astronomico di Brera sede di Merate, I-23807 Merate, Lecco, Italy*

[159]Departamento de Matemáticas, Universitat de València, E-46100 Burjassot, València, Spain
[160]Montana State University, Bozeman, MT 59717, USA
[161]The University of Utah, Salt Lake City, UT 84112, USA
[162]Johns Hopkins University, Baltimore, MD 21218, USA
[163]University of Rhode Island, Kingston, RI 02881, USA
[164]The University of Texas Rio Grande Valley, Brownsville, TX 78520, USA
[165]Université de Liège, B-4000 Liège, Belgium
[166]DIFA- Alma Mater Studiorum Università di Bologna, Via Zamboni, 33 - 40126 Bologna, Italy
[167]Istituto Nazionale Di Fisica Nucleare - Sezione di Bologna, viale Carlo Berti Pichat 6/2 - 40127 Bologna, Italy
[168]University of Manitoba, Winnipeg, MB R3T 2N2, Canada
[169]INFN-CNAF - Bologna, Viale Carlo Berti Pichat, 6/2, 40127 Bologna BO, Italy
[170]Università degli Studi di Sassari, I-07100 Sassari, Italy
[171]INFN, Laboratori Nazionali del Sud, I-95125 Catania, Italy
[172]Université de Normandie, ENSICAEN, UNICAEN, CNRS/IN2P3, LPC Caen, F-14000 Caen, France
[173]Laboratoire de Physique Corpusculaire Caen, 6 boulevard du maréchal Juin, F-14050 Caen, France
[174]The University of Sheffield, Sheffield S10 2TN, United Kingdom
[175]Université Claude Bernard Lyon 1, CNRS, Laboratoire des Matériaux Avancés (LMA), IP2I Lyon / IN2P3, UMR 5822, F-69622 Villeurbanne, France
[176]Università di Firenze, Sesto Fiorentino I-50019, Italy
[177]IGFAE, Universidade de Santiago de Compostela, E-15782 Santiago de Compostela, Spain
[178]Dipartimento di Scienze Matematiche, Fisiche e Informatiche, Università di Parma, I-43124 Parma, Italy
[179]INFN, Sezione di Milano Bicocca, Gruppo Collegato di Parma, I-43124 Parma, Italy
[180]California State University, Los Angeles, Los Angeles, CA 90032, USA
[181]Marquette University, Milwaukee, WI 53233, USA
[182]Perimeter Institute, Waterloo, ON N2L 2Y5, Canada
[183]Corps des Mines, Mines Paris, Université PSL, 60 Bd Saint-Michel, 75272 Paris, France
[184]Dipartimento di Fisica, Università di Trieste, I-34127 Trieste, Italy
[185]Université Côte d'Azur, Observatoire de la Côte d'Azur, CNRS, Lagrange, F-06304 Nice, France
[186]National Center for Nuclear Research, 05-400 Świerk-Otwock, Poland
[187]Vrije Universiteit Brussel, 1050 Brussel, Belgium
[188]University of Zurich, Winterthurerstrasse 190, 8057 Zurich, Switzerland
[189]Universidad de Antioquia, Medellín, Colombia
[190]Canadian Institute for Theoretical Astrophysics, University of Toronto, Toronto, ON M5S 3H8, Canada
[191]Stony Brook University, Stony Brook, NY 11794, USA
[192]Center for Computational Astrophysics, Flatiron Institute, New York, NY 10010, USA
[193]Montclair State University, Montclair, NJ 07043, USA
[194]HUN-REN Institute for Nuclear Research, H-4026 Debrecen, Hungary
[195]Indian Institute of Technology Bombay, Powai, Mumbai 400 076, India
[196]Centro de Física das Universidades do Minho e do Porto, Universidade do Minho, PT-4710-057 Braga, Portugal
[197]Aix Marseille Univ, CNRS/IN2P3, CPPM, Marseille, France
[198]CNR-SPIN, I-84084 Fisciano, Salerno, Italy
[199]Scuola di Ingegneria, Università della Basilicata, I-85100 Potenza, Italy
[200]Western Washington University, Bellingham, WA 98225, USA
[201]SUPA, University of the West of Scotland, Paisley PA1 2BE, United Kingdom
[202]Barry University, Miami Shores, FL 33168, USA
[203]Eötvös University, Budapest 1117, Hungary
[204]Institute for Cosmic Ray Research, KAGRA Observatory, The University of Tokyo, 5-1-5 Kashiwa-no-Ha, Kashiwa City, Chiba 277-8582, Japan
[205]Department of Physics, Graduate School of Science, Osaka Metropolitan University, 3-3-138 Sugimoto-cho, Sumiyoshi-ku, Osaka City, Osaka 558-8585, Japan
[206]University of Sannio at Benevento, I-82100 Benevento, Italy and INFN, Sezione di Napoli, I-80100 Napoli, Italy
[207]University of California, Berkeley, CA 94720, USA
[208]Instituto de Fisica Teorica UAM-CSIC, Universidad Autonoma de Madrid, 28049 Madrid, Spain
[209]Laboratoire d'Acoustique de l'Université du Mans, UMR CNRS 6613, F-72085 Le Mans, France
[210]University of Southampton, Southampton SO17 1BJ, United Kingdom
[211]University of California, Riverside, Riverside, CA 92521, USA
[212]Dipartimento di Ingegneria Industriale, Elettronica e Meccanica, Università degli Studi Roma Tre, I-00146 Roma, Italy

[213] University of Nevada, Las Vegas, Las Vegas, NV 89154, USA
[214] University of Nottingham NG7 2RD, UK
[215] Ariel University, Ramat HaGolan St 65, Ari'el, Israel
[216] The University of Mississippi, University, MS 38677, USA
[217] Graduate School of Science, Institute of Science Tokyo,
2-12-1 Ookayama, Meguro-ku, Tokyo 152-8551, Japan
[218] Institute of Physics, Academia Sinica, 128 Sec. 2, Academia Rd., Nankang, Taipei 11529, Taiwan
[219] The Chinese University of Hong Kong, Shatin, NT, Hong Kong
[220] American University, Washington, DC 20016, USA
[221] Dipartimento di Fisica, Università degli studi di Milano, Via Celoria 16, I-20133, Milano, Italy
[222] INFN, sezione di Milano, Via Celoria 16, I-20133, Milano, Italy
[223] Department of Applied Physics, Fukuoka University,
8-19-1 Nanakuma, Jonan, Fukuoka City, Fukuoka 814-0180, Japan
[224] University of Cambridge, Cambridge CB2 1TN, United Kingdom
[225] University of Lancaster, Lancaster LA1 4YW, United Kingdom
[226] College of Industrial Technology, Nihon University,
1-2-1 Izumi, Narashino City, Chiba 275-8575, Japan
[227] Faculty of Engineering, Niigata University, 8050 Ikarashi-2-no-cho, Nishi-ku, Niigata City, Niigata 950-2181, Japan
[228] Department of Physics, Tamkang University, No. 151,
Yingzhuan Rd., Danshui Dist., New Taipei City 25137, Taiwan
[229] Rutherford Appleton Laboratory, Didcot OX11 0DE, United Kingdom
[230] Department of Physical Sciences, Aoyama Gakuin University,
5-10-1 Fuchinobe, Sagamihara City, Kanagawa 252-5258, Japan
[231] Helmut Schmidt University, D-22043 Hamburg, Germany
[232] Nambu Yoichiro Institute of Theoretical and Experimental Physics (NITEP),
Osaka Metropolitan University, 3-3-138 Sugimoto-cho,
Sumiyoshi-ku, Osaka City, Osaka 558-8585, Japan
[233] Directorate of Construction, Services & Estate Management, Mumbai 400094, India
[234] Observatoire Astronomique de Strasbourg, 11 Rue de l'Université, 67000 Strasbourg, France
[235] Faculty of Physics, University of Białystok, 15-245 Białystok, Poland
[236] National Astronomical Observatories, Chinese Academic of Sciences,
20A Datun Road, Chaoyang District, Beijing, China
[237] School of Astronomy and Space Science, University of Chinese Academy of Sciences,
20A Datun Road, Chaoyang District, Beijing, China
[238] Sungkyunkwan University, Seoul 03063, Republic of Korea
[239] Department of Physics, Ulsan National Institute of Science and Technology (UNIST),
50 UNIST-gil, Ulju-gun, Ulsan 44919, Republic of Korea
[240] Institute for Cosmic Ray Research, The University of Tokyo,
5-1-5 Kashiwa-no-Ha, Kashiwa City, Chiba 277-8582, Japan
[241] Chung-Ang University, Seoul 06974, Republic of Korea
[242] University of Washington Bothell, Bothell, WA 98011, USA
[243] Laboratoire de Physique et de Chimie de l'Environnement,
Université Joseph KI-ZERBO, 9GH2+3V5, Ouagadougou, Burkina Faso
[244] Ewha Womans University, Seoul 03760, Republic of Korea
[245] National Institute for Mathematical Sciences, Daejeon 34047, Republic of Korea
[246] Korea Astronomy and Space Science Institute, Daejeon 34055, Republic of Korea
[247] Department of Astronomy and Space Science, Chungnam National University,
9 Daehak-ro, Yuseong-gu, Daejeon 34134, Republic of Korea
[248] Institute of Particle and Nuclear Studies (IPNS),
High Energy Accelerator Research Organization (KEK),
1-1 Oho, Tsukuba City, Ibaraki 305-0801, Japan
[249] Division of Science, National Astronomical Observatory of Japan,
2-21-1 Osawa, Mitaka City, Tokyo 181-8588, Japan
[250] Nagoya University, Nagoya, 464-8601, Japan
[251] Department of Physics, Aristotle University of Thessaloniki, 54124 Thessaloniki, Greece
[252] Bard College, Annandale-On-Hudson, NY 12504, USA
[253] Technical University of Braunschweig, D-38106 Braunschweig, Germany
[254] Institute of Mathematics, Polish Academy of Sciences, 00656 Warsaw, Poland
[255] Astronomical Observatory, Jagiellonian University, 31-007 Cracow, Poland
[256] Department of Physics and Astronomy, University of Padova, Via Marzolo, 8-35151 Padova, Italy
[257] Sezione di Padova, Istituto Nazionale di Fisica Nucleare (INFN), Via Marzolo, 8-35131 Padova, Italy
[258] Department of Physics, Nagoya University, ES building,
Furocho, Chikusa-ku, Nagoya, Aichi 464-8602, Japan
[259] Université de Montréal/Polytechnique, Montreal, Quebec H3T 1J4, Canada

[260]Indian Institute of Science Education and Research, Kolkata, Mohanpur, West Bengal 741252, India
[261]Seoul National University, Seoul 08826, Republic of Korea
[262]Department of Computer Simulation, Inje University,
197 Inje-ro, Gimhae, Gyeongsangnam-do 50834, Republic of Korea
[263]NAVIER, École des Ponts, Univ Gustave Eiffel, CNRS, Marne-la-Vallée, France
[264]Gravitational Wave Science Project, National Astronomical
Observatory of Japan (NAOJ), Mitaka City, Tokyo 181-8588, Japan
[265]Department of Physics, National Cheng Kung University,
No.1, University Road, Tainan City 701, Taiwan
[266]St. Thomas University, Miami Gardens, FL 33054, USA
[267]Scuola Normale Superiore, I-56126 Pisa, Italy
[268]Institució Catalana de Recerca i Estudis Avançats, E-08010 Barcelona, Spain
[269]Institut de Física d'Altes Energies, E-08193 Barcelona, Spain
[270]Institut fuer Theoretische Astrophysik, Zentrum fuer Astronomie Heidelberg,
Universitaet Heidelberg, Albert Ueberle Str. 2, 69120 Heidelberg, Germany
[271]Institucio Catalana de Recerca i Estudis Avançats (ICREA),
Passeig de Lluís Companys, 23, 08010 Barcelona, Spain
[272]Research Center for Space Science, Advanced Research Laboratories, Tokyo City University,
3-3-1 Ushikubo-Nishi, Tsuzuki-Ku, Yokohama, Kanagawa 224-8551, Japan
[273]Tsinghua University, Beijing 100084, China
[274]Institut des Hautes Etudes Scientifiques, F-91440 Bures-sur-Yvette, France
[275]Faculty of Law, Ryukoku University, 67 Fukakusa Tsukamoto-cho,
Fushimi-ku, Kyoto City, Kyoto 612-8577, Japan
[276]Phenikaa Institute for Advanced Study (PIAS),
Phenikaa University, Yen Nghia, Ha Dong, Hanoi, Vietnam
[277]University of Stavanger, 4021 Stavanger, Norway
[278]Physics Program, Graduate School of Advanced Science and Engineering,
Hiroshima University, 1-3-1 Kagamiyama, Higashihiroshima City, Hiroshima 739-8526, Japan
[279]GRAPPA, Anton Pannekoek Institute for Astronomy and Institute for High-Energy Physics,
University of Amsterdam, 1098 XH Amsterdam, Netherlands
[280]University College London, London WC1E 6BT, United Kingdom
[281]Observatoire de Paris, 75014 Paris, France
[282]Laboratoire Univers et Théories, Observatoire de Paris, 92190 Meudon, France
[283]Graduate School of Science and Technology, Niigata University,
8050 Ikarashi-2-no-cho, Nishi-ku, Niigata City, Niigata 950-2181, Japan
[284]University of Maryland, Baltimore County, Baltimore, MD 21250, USA
[285]CSIR-Central Glass and Ceramic Research Institute, Kolkata, West Bengal 700032, India
[286]Consiglio Nazionale delle Ricerche - Istituto dei Sistemi Complessi, I-00185 Roma, Italy
[287]Department of Astronomy, Yonsei University,
50 Yonsei-Ro, Seodaemun-Gu, Seoul 03722, Republic of Korea
[288]Department of Physics, University of Guadalajara, Av. Revolucion 1500,
Colonia Olimpica C.P. 44430, Guadalajara, Jalisco, Mexico
[289]Hobart and William Smith Colleges, Geneva, NY 14456, USA
[290]INAF, Osservatorio Astronomico di Padova, I-35122 Padova, Italy
[291]Dipartimento di Ingegneria, Università del Sannio, I-82100 Benevento, Italy
[292]Museo Storico della Fisica e Centro Studi e Ricerche "Enrico Fermi", I-00184 Roma, Italy
[293]Kennesaw State University, Kennesaw, GA 30144, USA
[294]Subatech, CNRS/IN2P3 - IMT Atlantique - Nantes Université,
4 rue Alfred Kastler BP 20722 44307 Nantes CÉDEX 03, France
[295]Departamento de Física - ETSIDI, Universidad Politécnica de Madrid, 28012 Madrid, Spain
[296]Department of Electronic Control Engineering,
National Institute of Technology, Nagaoka College,
888 Nishikatakai, Nagaoka City, Niigata 940-8532, Japan
[297]Trinity College, Hartford, CT 06106, USA
[298]Dipartimento di Fisica e Scienze della Terra, Università Degli Studi di Ferrara, Via Saragat, 1, 44121 Ferrara FE, Italy
[299]Faculty of Science, Toho University, 2-2-1 Miyama, Funabashi City, Chiba 274-8510, Japan
[300]Indian Institute of Technology, Palaj, Gandhinagar, Gujarat 382355, India
[301]Kavli Institute for Astronomy and Astrophysics, Peking University,
Yiheyuan Road 5, Haidian District, Beijing 100871, China
[302]Laboratoire MSME, Cité Descartes, 5 Boulevard Descartes,
Champs-sur-Marne, 77454 Marne-la-Vallée Cedex 2, France
[303]Faculty of Information Science and Technology, Osaka Institute of Technology,
1-79-1 Kitayama, Hirakata City, Osaka 573-0196, Japan

[304] NASA Goddard Space Flight Center, Greenbelt, MD 20771, USA
[305] Faculty of Science and Technology, Kochi University, 2-5-1 Akebono-cho, Kochi-shi, Kochi 780-8520, Japan
[306] Laboratoire de Physique de l'École Normale Supérieure, ENS, (CNRS, Université PSL, Sorbonne Université, Université Paris Cité), F-75005 Paris, France
[307] Faculty of Physics, University of Warsaw, Ludwika Pasteura 5, 02-093 Warszawa, Poland
[308] Laser Interferometry and Gravitational Wave Astronomy, Max Planck Institute for Gravitational Physics, Callinstrasse 38, 30167 Hannover, Germany
[309] The Hakubi Center for Advanced Research, Kyoto University, Yoshida-honmachi, Sakyou-ku, Kyoto City, Kyoto 606-8501, Japan
[310] Department of Physics, Kyoto University, Kita-Shirakawa Oiwake-cho, Sakyou-ku, Kyoto City, Kyoto 606-8502, Japan
[311] Yukawa Institute for Theoretical Physics (YITP), Kyoto University, Kita-Shirakawa Oiwake-cho, Sakyou-ku, Kyoto City, Kyoto 606-8502, Japan
[312] University of Catania, Department of Physics and Astronomy, Via S. Sofia, 64, 95123 Catania CT, Italy
[313] National Institute of Technology, Fukui College, Geshi-cho, Sabae-shi, Fukui 916-8507, Japan
[314] Department of Communications Engineering, National Defense Academy of Japan, 1-10-20 Hashirimizu, Yokosuka City, Kanagawa 239-8686, Japan
[315] Eindhoven University of Technology, 5600 MB Eindhoven, Netherlands
[316] Department of Physics and Astronomy, University of North Carolina at Chapel Hill, 120 E. Cameron Ave, Chapel Hill, NC, 27599, USA
[317] David A. Dunlap Department of Astronomy and Astrophysics, University of Toronto, 50 St George St, Toronto ON M5S 3H4, Canada
[318] Kavli Institute for the Physics and Mathematics of the Universe (Kavli IPMU), WPI, The University of Tokyo, 5-1-5 Kashiwa-no-Ha, Kashiwa City, Chiba 277-8583, Japan
[319] Department of Astronomy, Beijing Normal University, Xinjiekouwai Street 19, Haidian District, Beijing 100875, China
[320] School of Physics and Technology, Wuhan University, Bayi Road 299, Wuchang District, Wuhan, Hubei, 430072, China

We present results from the search for an isotropic gravitational-wave background using Advanced LIGO and Advanced Virgo data from O1 through O4a, the first part of the fourth observing run. This background is the accumulated signal from unresolved sources throughout cosmic history and encodes information about the merger history of compact binaries throughout the Universe, as well as exotic physics and potentially primordial processes from the early cosmos. Our cross-correlation analysis reveals no statistically significant background signal, enabling us to constrain several theoretical scenarios. For compact binary coalescences which approximately follow a 2/3 power-law spectrum, we constrain the fractional energy density to $\Omega_{\rm GW}(25\,{\rm Hz}) \leq 2.0 \times 10^{-9}$ (95% credibility), a factor of 1.7 improvement over previous results. Scale-invariant backgrounds are constrained to $\Omega_{\rm GW}(25\,{\rm Hz}) \leq 2.8 \times 10^{-9}$, representing a 2.1× sensitivity gain. We also place new limits on alternative gravity theories predicting non-standard polarization modes and confirm that terrestrial magnetic noise sources remain below our detection threshold. Combining these spectral limits with population models for GWTC-4, the latest gravitational-wave event catalog, we find our constraints remain above predicted merger backgrounds but are approaching detectability. The joint analysis combining the background limits shown here with the GWTC-4 catalog enables improved inference of the binary black hole merger rate evolution across cosmic time. Furthermore, employing GWTC-4 inference results and standard modeling choices, we estimate that the total background arising from compact binary coalescences is $\Omega_{\rm CBC}(25{\rm Hz}) = 0.9^{+1.1}_{-0.5} \times 10^{-9}$ at 90% confidence, where the largest contribution is due to binary black holes only, $\Omega_{\rm BBH}(25\,{\rm Hz}) = 0.8^{+1.1}_{-0.5} \times 10^{-9}$.

I. INTRODUCTION

The superposition of individually unresolved gravitational-wave (GW) signals accumulated throughout cosmic history gives rise to a gravitational-wave background (GWB) [1, 2] which produces a persistent incoherent signal in GW detectors. The GWB is commonly referred to as "stochastic" as it can be characterized statistically as a mean zero stochastic field [1].

GWB sources can be categorized as cosmological or astrophysical based on their origin. The former provides a unique probe of the early Universe, as GWs propagate directly from the inflationary epoch, while the latter results from an ensemble of unresolved astrophysical events, offering insights into source populations at high redshift. Potential contributors to the GWB include distant unresolved compact binary mergers [3–7], core-collapse supernovae [3, 7–9], rotating neutron stars [8–14], stellar core collapse [15, 16] and superradiance of axion clouds around black holes [17–21]. Some of the cosmological sources are cosmic strings [22–35], first-order phase tran-

* Deceased, September 2024.

sitions in the early Universe [36–44], primordial black holes [45–52], a stiff equation of state in the early Universe [53–58], and gravitational waves generated during inflation [59–69].

The Laser Interferometer Gravitational-wave Observatory (LIGO) [70], Virgo [71], and KAGRA [72] collaborations (LVK collaborations [73]) have previously placed upper limits on both isotropic [74] and anisotropic [75] GWBs using data from the first three observing runs collected by the LIGO Hanford, LIGO Livingston, and Virgo interferometers. These searches relied on cross-correlating data between detector pairs [1]. The implications of the upper limits placed on the GWB energy density spectrum with LVK data have been far-reaching, setting competitive bounds on early Universe physics [26, 27, 43, 44, 50, 51, 58, 65], and expanding our knowledge of the astrophysical binary population properties complementary to what is obtained from individual GW sources [74, 76–78].

The most compelling astrophysical sources of a GWB in our detector range are compact binary coalescences (CBCs). The CBC background is expected to be an approximately isotropic [79–81] spectral power-law signal, peaking around a few hundred Hz (depending on the features of the CBC population [81–84]). The signal is not expected to be Gaussian due to the intermittent nature of the background, in the frequency range probed [85]. In this work, we update our models to estimate the expected contributions from binary black holes (BBHs), binary neutron stars (BNSs) and neutron star-black hole (NSBH) coalescences, incorporating the most recent observational data from O4a [86–89]. For the BBH population in particular, we adopt the methodology of [76] to constrain the redshift-dependent merger rate by combining individually resolved events with upper limits from the cross-correlation analysis presented in this paper. This approach allows us to construct a full posterior distribution for the resulting energy density spectrum, accounting for current uncertainties in the mass, spin and redshift distributions of the BBH population. Additionally, by combining the contributions from all classes of CBCs and comparing the resulting GWB spectrum with the projected sensitivity curves of the upgraded Advanced LIGO detectors (A+) [90] and Virgo detector (V+) [91], we demonstrate that one year of time-coincident data between detectors in the network at design sensitivity would enable us to substantially probe and potentially detect the expected signal arising from the CBC population.

In this work we follow the same methodology as previous observing runs, cross-correlating data from LIGO Hanford and Livingston detectors during the first portion of the fourth observing run, hereinafter referred to as O4a. During this first part of the run, Virgo was not in science mode, hence why it is not included in our analysis. In this paper, we focus exclusively on the isotropic GWB, while complementary results from an anisotropic search are presented in a companion paper [92]. The cross-correlation search method employed is optimal for a continuous Gaussian signal, given appropriate caveats [1, 93], while it is sub-optimal but still sensitive to an intermittent signal [94]. Several alternative search methods are currently being explored tailored to intermittent signals [94–97].

As we do not detect a GWB, we set upper limits on its amplitude. We include inference on a set of possible GWB models, including an astrophysical signal sourced by CBCs and alternative GWB polarization modes [98] arising in theories of gravity beyond General Relativity (GR). As in O3, loud glitches are excluded from the analysis [99, 100]. Additionally, as correlated magnetic noise is a potential limiting factor in stochastic background searches especially as detector sensitivity improves, we construct a magnetic noise budget, and find it lies well below the current GWB sensitivity. Alongside this paper, the LVK collaboration is also releasing a companion paper exploring the cosmological implications of our results [101], focusing on the constraints these place on potential early-Universe sources of the GWB.

This paper is organized as follows. In Section II, we outline the analysis methods employed throughout. Section III details the procedures implemented to remove identifiable sources of detector artifacts that can bias the results and implications of the search. Section IV presents the results of our analysis. Finally, in Section V, we discuss the astrophysical implications of our findings and provide constraints on the BBH merger rate.

II. METHODS

The isotropic stochastic analysis presented here targets the spectral properties of the GWB, modeling the signal as isotropic, unpolarized, stationary, and Gaussian in the limit of long observing time [1, 102]. The signal is also assumed to be weak with respect to the detector sensitivity [93].

The GWB spectrum may be expressed in terms of the fractional GW energy density spectrum $\Omega_{\rm GW}(f)$, defined as

$$\Omega_{\rm GW}(f) = \frac{1}{\rho_{\rm c}} \frac{{\rm d}\rho_{\rm GW}(f)}{{\rm d}\ln f}\,, \tag{1}$$

where ${\rm d}\rho_{\rm GW}$ is the GW energy density in the frequency band $[f, f + {\rm d}f]$, and $\rho_{\rm c} = 3H_0^2c^2/(8\pi G)$ is the critical energy density in the Universe, with c the speed of light and G Newtons constant. Integrating $\Omega_{\rm GW}(f)$ over ${\rm d}\ln f$ returns the total dimensionless GW energy density. In what follows, we adopt the Planck 2015 cosmological parameters, fixing the Hubble constant to $H_0 = 67.9\,{\rm km\,s^{-1}\,Mpc^{-1}}$ and the present-day matter density parameter to $\Omega_{\rm m,0} = 0.3065$ [103].

The analysis presented is carried out with the `pygwb` analysis package [104, 105]. In the following we summarize the methodological approach and specific choices made in the analysis of the O4a dataset. Methods employed here do not vary significantly from those of previous observing runs O1 [106], O2 [107], and O3 [74], so that the resulting spectra may be ultimately combined into a single result. Changes with respect to previous analyses are highlighted in the text.

A. Cross-correlation spectra

Following [108], we employ cross-correlation spectra calculated from pairs of independent, time-coincident detector strain datastreams to construct an estimator for $\Omega_{\rm GW}(f)$:

$$\hat{\Omega}_0(f) = \frac{\mathrm{Re}[C_{IJ}(f)]}{\gamma_{IJ}(f)S_0(f)}\,, \tag{2}$$

where C_{IJ} is the cross-spectral density (CSD) calculated from the Fourier-transformed strain data $\tilde{s}(f)$ of duration T from two non-coincident detectors I and J:

$$C_{IJ}(f) = \frac{2}{T}\tilde{s}^*_I(f)\tilde{s}_J(f). \tag{3}$$

The geometric quantity $\gamma_{IJ}(f)$ is referred to as the overlap reduction function (ORF) [1, 109], which quantifies the frequency-dependent decoherence that affects the cross-correlation of data from two geographically separated interferometers. This reduction depends on the individual detector responses as well as their relative separation and orientation [1]. The function $S_0(f)$ converts units of GW strain power into fractional energy density, whilst encoding also a frequency weighting specific to a chosen spectral model $F_0(f)$:

$$S_0(f) = \frac{3H_0^2F_0^2(f)}{10\pi^2}\frac{1}{f^3}\,. \tag{4}$$

As discussed in [93], in the case of noise-dominated data streams the cross-correlation statistic described above is a quasi-optimal [1] estimator for the background spectrum.

In line with previous analyses [74, 106, 107], here we assume a power-law spectral model expressed as an amplitude Ω_α with respect to the fixed reference frequency $f_{\rm ref} = 25\,\mathrm{Hz}$ scaling with a power-law index α,

$$\Omega_{\rm GW}(f) = \Omega_\alpha F_\alpha(f)\,, \qquad F_\alpha(f) = \left(\frac{f}{25\,\mathrm{Hz}}\right)^\alpha. \tag{5}$$

In Eq. (2) specifically, the chosen spectral model is fixed to a power law with spectral index $\alpha = 0$, as indicated by the subscript of S_0 and that of the estimator in Eq. (2).

[1] Sub-optimality is due to corrections to the variance Eq. (6) of the same order of magnitude of the signal, which become negligible when the signal is weak compared to the detector noise.

The corresponding variance estimate is [1]

$$\sigma_0^2(f) = \frac{1}{2T\Delta f}\frac{P_I(f)P_J(f)}{\gamma_{IJ}^2(f)S_0^2(f)}\,, \tag{6}$$

where $P_I(f)$ is the one-sided power spectral density for detector I, and Δf is the frequency resolution employed in the analysis.

In practice, due to noise non-stationarities and computational efficiency the $\hat{\Omega}_0(f)$ spectrum is estimated from a weighted average over a large number of data segments, where for each time segment i there is a corresponding CSD estimate $C_{IJ,\,i}$ and PSD estimates $P_{I,\,i}$, $P_{J,\,i}$. Further details about this cross-correlation computation may be found in the `pygwb` publication [104].

B. Frequency estimator

We construct a narrow-band estimator $\hat{\Omega}_0(f)$ with associated variance $\sigma_0^2(f)$:

$$\hat{\Omega}_0(f) = \frac{\sum_i\left[\hat{\Omega}_0(f;t_i)\sigma_0^{-2}(f;t_i)\right]}{\sum_i\sigma_0^{-2}(f;t_i)}\,, \tag{7}$$

$$\sigma_0(f) = \left[\sum_i\sigma_0^{-2}(f;t_i)\right]^{-1/2}\,, \tag{8}$$

where i labels data from t_i to $t_i + \Delta t$. In practice, the cross-spectral densities are calculated from the data with a 50% overlap to make up for the impact of Hann-windowing each segment, hence each independent time estimate is achieved by handling even and odd segments separately as described in [104].

This calculation is performed employing the $S_0(f)$ weighting function. However, note that it can be performed by choosing any other power-law weighting α, and it is possible to re-weight from one index, α_1, to another, α_2, as

$$\hat{\Omega}_{\alpha_1}(f) = \hat{\Omega}_{\alpha_2}(f)\frac{F_{\alpha_1}(f)}{F_{\alpha_2}(f)}\,. \tag{9}$$

Broadband estimates for a spectral index α and at reference frequency 25 Hz are obtained by optimally weighting the narrowband estimator, as described in [74, 104]:

$$\hat{\Omega}_\alpha|_{25\,\mathrm{Hz}} = \frac{\sum_f\hat{\Omega}_0(f)F_\alpha(f)\sigma_0^{-2}(f)}{\sum_f F_\alpha^2(f)\sigma_0^{-2}(f)}\,, \tag{10}$$

$$\sigma_\alpha|_{25\,\mathrm{Hz}} = \left[\sum_f F_\alpha(f)\sigma_0^{-2}(f)\right]^{-1/2}\,. \tag{11}$$

C. Parameter estimation

Parameter estimation is performed here using a hybrid approach that combines frequentist and Bayesian analysis techniques [110]. Specifically, the frequentist estimators from the previous sections, $\hat{\Omega}_0(f)$ and $\sigma_0(f)$, combined over the entire observing period, are used as input data to calculate posterior probability distributions of GWB model parameters. These in turn are used to compute upper bounds on the spectral amplitude of the GWB. In [93] the authors show that in the weak-signal approximation this hybrid approach does not lose information compared to a fully Bayesian search, which produces posterior distributions from the full time series data rather than from the time-averaged frequency estimators.

We assume that, in each frequency bin, the unweighted spectral estimate $\hat{\Omega}_0$ is Gaussian-distributed with variance σ_0^2 [74]:

$$p(\hat{\Omega}_0|\Theta) \propto \exp\left[-\frac{1}{2}\sum_f \frac{(\hat{\Omega}_0(f) - \Omega_{\rm GW}(f;\Theta))^2}{\sigma_0^2(f)}\right], \quad (12)$$

where $\Omega_{\rm GW}(f;\Theta)$ is an assumed model for the GWB signal, parametrized via a set of model parameters Θ. Posteriors for the model parameters Θ are obtained by employing the `pygwb` library [104] and the `Bilby` library [111] for detector modeling and likelihood evaluation. As in previous work, e.g. [74], this analysis is performed using data from multiple detector pairs, I, J (i.e., *baselines*). Data from different baselines are assumed to be independent, such that the combined inference assumes likelihood (12) holds for data from each individual baseline, $\hat{\Omega}_0^{IJ}(f)$, $\sigma_0^{IJ}(f)$, and the total likelihood is the result of the product of the likelihood calculated for each baseline.

We consider different models for the GWB:

- Noise: $\Omega_{\rm GW}(f;\Theta) = 0$. We implicitly include uncorrelated Gaussian noise as part of every model that follows in the prior choices for the model parameters. This noise model is not strictly correct as there are potential sources of correlated noise, such as Schumann resonances [112]. However, these effects may be neglected in the present search due to detector sensitivity, as shown in Sec. III F.

- Power law: $\Omega_{\rm GW}(f;\Theta) = \Omega_{\rm ref} F_\alpha(f)$, as per Eq. (5). In this analysis, the two parameters $\Theta = \{\Omega_{\rm ref}, \alpha\}$ are inferred independently, and hence we choose this notation to avoid confusion with the cross-correlation estimators described above. The reference frequency is set to $f_{\rm ref} = 25\,{\rm Hz}$ as in past analyses [74] due to the location of peak stochastic sensitivity, for lower values of α. Note that the precise sensitivity depends on the spectral index α.

- Scalar-vector-tensor (SVT) power law: this model assumes that the signal may include vector and scalar polarizations as well as the standard tensor polarization predicted by General Relativity. This background is modeled as a superposition of individual contributions, labeled $({\rm p}) = \{{\rm T}, {\rm V}, {\rm S}\}$ where each component is individually modeled by a power law [113]:

$$\Omega_{\rm GW}(f;\Theta) = \sum_{({\rm p})} \beta^{({\rm p})}(f)\Omega_{\rm ref}^{({\rm p})} F_{\alpha_{\rm p}}(f), \quad (13)$$

where $\beta^{({\rm p})}(f) \equiv \gamma_{IJ}^{({\rm p})}(f)/\gamma_{IJ}(f)$ is the ratio between the ORF for polarization (p) and the standard (tensor) polarization [98].

- Magnetic: describes correlations between pairs of detectors induced by large-scale coherent magnetic fields that can mimic a GWB signal. These are modeled in terms of magnetometer correlations and a transfer function between the local magnetic field and the strain channel of the detectors. Further discussion on this model is given in section IV D.

- Compact binary coalescences (CBC): the predominant contribution to the GWB is expected to be the superposition of all merging compact binaries in the observable Universe [82]. The total GW fractional energy density due to compact binary mergers, $\Omega_{\rm CBC}$, can be parametrized as a function of the mass distribution of compact binaries and their merger rate as a function of redshift. This model will be discussed in Section V. Assuming $\Omega_{\rm CBC}$ is the only contributor to the stochastic signal in the analyzed frequency band, we can infer mass and merger rate population parameters.

To test these different models against the data, we calculate Bayes factors for each model. Unless otherwise specified, we compute the Bayes factor between the hypothesis of a specific signal model with respect to the noise model, $\Omega_{\rm GW}(f;\Theta) \equiv 0$.

III. DATA QUALITY

This section describes the data quality and handling specifics for the strain data collected during the first portion of the fourth observing run (O4a) by the LIGO Hanford and Livingston detectors. Note that results presented in the following sections include the combination of this data with previous datasets O1, O2, O3, whose relevant instrument performances and data quality features are described in [114–117], [118–120], [121–124] respectively. The O3 analysis also includes data from Virgo [125–130]. For further details on the performance of the LIGO detectors and the quality of their data during O4a [131, 132], see also [133].

A. Data

The O4a observing period ran from 15:00 UTC on May 24, 2023 to 16:00 UTC on January 16, 2024. The total coincident time for the Hanford-Livingston (HL) baseline in this period was 126.57 days, before applying data quality cuts. The strain data used in this analysis were calibrated strain data with narrow-band features from photon calibrator and actuation injections and power mains noise, subtracted [134], followed by the application of non-stationary noise subtraction [135]. The correlated magnetic noise was monitored using low-noise LEMI120 magnetometers located at each site [136]. The same data processing was carried out for both strain and magnetometer data to allow a comparison between the magnetic and GW analyses.

Both strain and magnetic datastreams are initially downsampled from the original sample rate of 16384 Hz to 4096 Hz. This downsampling is used because the GW sources targeted in this search populate frequencies below 2 kHz. The data are high-pass filtered using a 16th-order Butterworth filter with a knee frequency of 11 Hz, which is constructed using second-order sections. As in analyses described in [74, 104], each data stream is divided into 50% overlapping, Hann-windowed 192-second segments, coarse-grained to a frequency resolution of 1/32 Hz. The analyzed frequency range spans $20 - 1726$ Hz; the minimum frequency is chosen based on the detector sensitivities [133], while the maximum frequency is chosen to be sufficiently below the Nyquist frequency to avoid aliasing effects.

In the following text, tables, and figures, we label the LIGO Hanford detector as LHO and the LIGO Livingston as LLO.

B. Time domain cuts: vetoed times

Data quality for analysis purposes was assessed jointly with the Detector Characterization groups of LIGO, Virgo, and KAGRA. Data quality flags are employed to define observing time periods to be vetoed from analysis. Most significant to this search are the "Category 1" vetoes. These vetoes correspond to times when the detector was known to be operating outside of its nominal condition. For more details on the O4a data quality and the specific time-domain cuts made for stochastic data quality purposes, please refer to [133], Sec. 4.3. After applying vetoes, the remaining viable time-coincident data is 126.47 days. The relevant segment information used to exclude vetoed data from this analysis will be available on GWOSC [137].

C. Time domain cuts: gating

In the third LVK observing run (O3), a large population of loud glitches [74] led to very frequent flagging of data segments by non-stationarity checks (see Sec. III D). To mitigate this effect, time-domain gating of the data was introduced [138, 139]: loud glitches are removed from the data stream by multiplying the data with an inverse Planck-taper window with parameters tailored to the specific non-stationary feature (e.g., duration) [140].

In O4a, data are preprocessed with an auto-gating procedure as described in [105]. The parameters chosen for the auto-gating were optimized for this specific search, minimizing the amount of data lost whilst retaining stationarity. A total of 0.093% of analyzed Hanford data and 0.068% of Livingston data were gated; more details can be found in Sec. 4.3.2. of [133].

D. Time domain cuts: stationarity checks

As in previous runs, we apply a non-stationarity cut (often referred to as the $\Delta\sigma$ cut [104]) by removing times where the square root of the variance in Eq. (6) is found to vary by more than 20% between neighbouring segments. We cut the union of segments that do not satisfy the stationarity test assuming a set of different spectral weights: $\alpha = \{-5, 0, 3, 5\}$, implemented as in Eq. (2). As each power law accumulates SNR in a different frequency band, these may flag different segments depending on their specific spectral narrowband/broadband features. This cut additionally removes 8.1% of the analysed segments, leaving 108.41 days of viable data.

E. Frequency domain cuts: narrowband features

In addition to broadband features that determine the exclusion of entire data segments from the analysis, also narrowband deviations from Gaussianity are investigated, and data cuts are applied to exclude problematic frequency bins. These frequencies are determined by monitoring the coherence between the GW channels at different sites, and between the GW channel and auxiliary channels at the same site. Bins that show evidence of instrumental noise or that manifest strong non-Gaussian behavior are excluded from the analysis: for more details, see [133], Sec. 2.1. The list of problematic frequencies, i.e., the *notch list*, is determined at the end of the observing run and then applied identically throughout the entire data analysis process (with a small exception in parameter estimation, as discussed in Sec. IV B). This list is included in the appended data release.

The notches include the following components:

- Calibration lines: these are stationary lines injected into each detector's differential arm feedback loop so as to continually monitor the detector response and the corresponding calibration amplitude factor. These include the stationary calibration lines injected throughout O4a [141], and one calibration line at 24.5 Hz that was turned on between July 25, 2023, and August 9, 2023.

- Pulsar injections: each injection corresponds to a simulation of a quasi-monochromatic, persistent GW signal as expected from a rapidly rotating, isolated neutron star. These were injected throughout the entire O4a run at both LIGO sites and emulate how canonical continuous-wave (CW) signals would appear in the detectors [142].

- Quadruple suspension violin modes: resonances of the detector mirror suspension fibers [70].

- Powerline harmonics: integer harmonics of the 60 Hz power mains present at both detectors.

- Other artifacts: DuoTone signals (960Hz, 961Hz) and their 1 Hz side band present in both LIGO detectors in O4a from the timing system, used to synchronize data collection across the global detector network and in each interferometer [143].

Overall, the notch list cuts 8.4% of the spectrum; however, note that in the frequency range $[20, 300]$ Hz where the detectors are most sensitive, only 2.7% of the spectrum is cut.

F. Magnetic noise budget

Correlated magnetic noise present across multiple detectors is a probable hindrance for stochastic analyses [144–146]. Examples of such correlated magnetic noise are Schumann resonances [147, 148], standing waves in the cavity between the Earth's surface and the ionosphere that may be excited by lightning strikes; and at higher frequencies, $f > 100$ Hz, correlated fields from lightning strikes. Magnetic fields of any source couple to the detector via electric cables in the detector buildings or couple to the actuation magnets controlling the detector test mass mirrors [125].

Magnetic fields are monitored with sensitive probes placed outside the detector buildings to produce a magnetic "noise budget", quantifying the strength of correlated magnetic noise present across detectors, which is then compared to the sensitivity of the detector network to a stochastic signal [149]. If this budget becomes large enough, correlated magnetic fields can contribute to correlated noise which may mimic a signal in the stochastic analysis presented here.

We compute the magnetic correlated noise budget via

$$\hat{\Omega}_{\text{mag},\, IJ}(f) = \frac{2}{T}\frac{|T_I(f)|\,|T_J(f)|\,\sqrt{\sum_{ab}|\tilde{m}^{\star}_{I,a}(f)\tilde{m}_{J,b}(f)|^2}}{\gamma_{IJ}(f)S_0(f)}, \tag{14}$$

where $T_I(f)$ and $T_J(f)$ are the magnetic coupling functions of detectors I and J, and $\tilde{m}_{I,a}(f)$ is the Fourier-transformed magnetic data from the outside probes of detector I pointing in the direction a, which can be either along the X or Y arms of a detector, and its sum runs over the four possible combinations of a and b. Magnetic coupling functions consist of the product of two terms: an outside-to-inside coupling, T_{OTI}, and an inside-to-strain coupling, T_{ITS}. The T_{OTI} term is given by the ratio of the strength of a magnetic source measured outside the detector buildings to the strength of the same source measured inside the buildings, and reduces to an overall constant averaged over several independent measurements, while T_{ITS} is estimated via hardware injections as explained below. Uncertainties on these measurements include the uncertainty on the outside-to-inside coupling as measured in O3 at LLO, and, to be conservative, an intrinsic uncertainty factor of 2 as the magnetometers in the building (used for the measurements) are not located at the exact location where the magnetic field couples to the strain.

The T_{ITS} functions are estimated by each detector site team by injecting far-field magnetic fields within the detector building and measuring the response in the strain channel [112, 123, 125]. A value is recorded as a measurement when both the magnetometer sensor and strain channel amplitude spectral densities (ASDs) exceed their respective set thresholds; otherwise, if only the magnetometer ASD exceeds the threshold, the value is treated as an upper limit. The coupling function is interpolated to the frequencies of the computed magnetic CSD, $\text{Re}\,[\tilde{m}^{\star}_I(f)\tilde{m}_J(f)]$. This does not create any artifacts in the coupling functions as these have a finer frequency resolution than the CSD. We include a calibration factor in the magnetic CSDs[2] and take the quadrature sum of the magnetic CSDs of four baselines, one for every combination of the two outside magnetometers at each detector used for computing the budget, as a most conservative estimate. These quantities are then combined in Eq. (14) to produce the magnetic budget shown in Fig. 1. Here the red bands show the uncertainties on the budget, compared to the 2σ power-law integrated sensitivity (PI) curve [150], showing the sensitivity of our search to power-law backgrounds.

The final budget indicates that no correlated (magnetic) noise observation is expected. Some narrowband features are expected, such as the harmonics of the US power lines at 60 Hz, and the ORF zero-crossings (related to the fact that a single baseline was considered for this analysis).

While the magnetic budget computation in O3 was performed differently[3], we can compare the two budgets at an order-of-magnitude level. At lower frequencies $f < 60$ Hz, the O4a budget is consistently within the band of the O3 budget, but in a narrow frequency band $60\,\text{Hz} < f < 65$ Hz, the O4a budget becomes slightly larger than

[2] The calibration factor is an intrinsic conversion factor between the measured current in the magnetometers and the actual magnetic field.

[3] In O3, weekly magnetic couplings were used and, due to fluctuations, computing a budget every single week produces a wide uncertainty band instead of a single line [123].

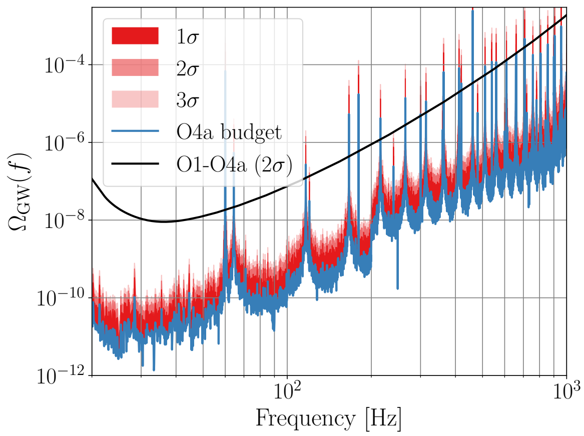

FIG. 1. The computed magnetic budget is shown in blue, including $\hat{\Omega}_{\rm mag} + 1\sigma$, $\hat{\Omega}_{\rm mag} + 2\sigma$, and $\hat{\Omega}_{\rm mag} + 3\sigma$ uncertainties (in progressively lighter shades of red). The magnetic budget remains consistently below the 2σ power-law integrated sensitivity curve (black), except for narrowband features numerically induced by the overlap reduction function (ORF) and harmonics of the 60 Hz power lines.

the maximum value in O3. This is related to a zero-crossing of the ORF virtually enhancing the magnetic budget due to its presence in the denominator of Eq. (14), and does not accurately represent a magnetic response of the detector and thus the actual magnetic budget in O4a. At higher frequencies $f > 65$ Hz, the O4a budget is broadly consistent with the O3 magnetic budget.

G. Calibration uncertainties

Calibration uncertainties account for both statistical uncertainties and systematic errors arising from the calibration process of LVK data[4] [151, 152]. These are incorporated in parameter estimation [104, 153] by introducing a Gaussian-distributed, positive-definite calibration factor Λ. As a result, the likelihood presented in Eq. (12) is modified as (see also App. B of [104])

$$p(\hat{\Omega}_0|\Theta, \Lambda) \propto \exp\left[-\frac{1}{2}\sum_f \frac{(\hat{\Omega}_0(f) - \Lambda\Omega_{\rm GW}(f;\Theta))^2}{\sigma_0^2(f)}\right], \tag{15}$$

where Λ is marginalized over, assuming the prior

$$p(\Lambda) = \frac{1}{\sqrt{2\pi\sigma_\Lambda^2}} \exp\left[-\frac{(\Lambda-1)^2}{2\sigma_\Lambda^2}\right]. \tag{16}$$

[4] Calibration is the procedure used to convert the digital output of a gravitational-wave detector into the relative displacement of the test masses within the detector.

The calibration variance σ_Λ is estimated in collaboration with the LIGO Calibration Group. Hourly calibration uncertainties provided by the Calibration Group are combined to obtain uncertainties in both the magnitude and phase of the strain at the 68% confidence level (CL). These uncertainties are frequency-dependent; however, we adopt a conservative approach and select the largest uncertainty across the entire frequency range for both magnitude and phase. The corresponding maximum uncertainties are summarized in Table I.

Interferometer	LHO	LLO
Magnitude	6.9%	4.1%
Phase	4.3°	5.1°

TABLE I. Maximum calibration uncertainties on the magnitude and phase of detector strain at 68% confidence level (CL), for the LIGO Hanford (LHO) and LIGO Livingston (LLO) detectors.

Provided it remains approximately below 5 degrees, the phase uncertainty does not introduce a significant bias in stochastic background estimates [154]. Hence we restrict the calculation of calibration uncertainty to the magnitude term only, taking the quadrature sum of the magnitude uncertainties for each detector strain. This yields a final value of $\sigma_\Lambda = 8.1\%$.

IV. RESULTS

We present results obtained with the analysis methods described above using data from the O4a observing run combined with data from the O1−O3 observing runs. We do not find evidence of a background signal in our analyses, as outlined below, hence we set upper limits on several models. We perform three different analyses: (i) we calculate the point estimate spectrum and variance of the GWB signal using cross-correlation optimal filtering (Sec. IV A) and set upper limits (Sec. IV B) considering a power-law spectral model for the overall background, both in the case of a fixed known spectral index α, and marginalizing over α; (ii) we set upper limits on SVT model parameters (Sec. IV C); and (iii) we perform joint inference in the case where a correlated magnetic signal is present in the data together with a GWB (Sec. IV D).

A. Cross-correlation estimates

We produce broadband estimates $\hat{\Omega}_\alpha$ and associated variance using an optimal filter for three different power-law models motivated by different potential GWB sources:

- $\alpha = 0$ corresponds to a scale-invariant signal, which approximately describes a GWB arising from a cosmic string network [26, 155–158] or slow-roll inflation [64, 159, 160] in the LVK frequency band.

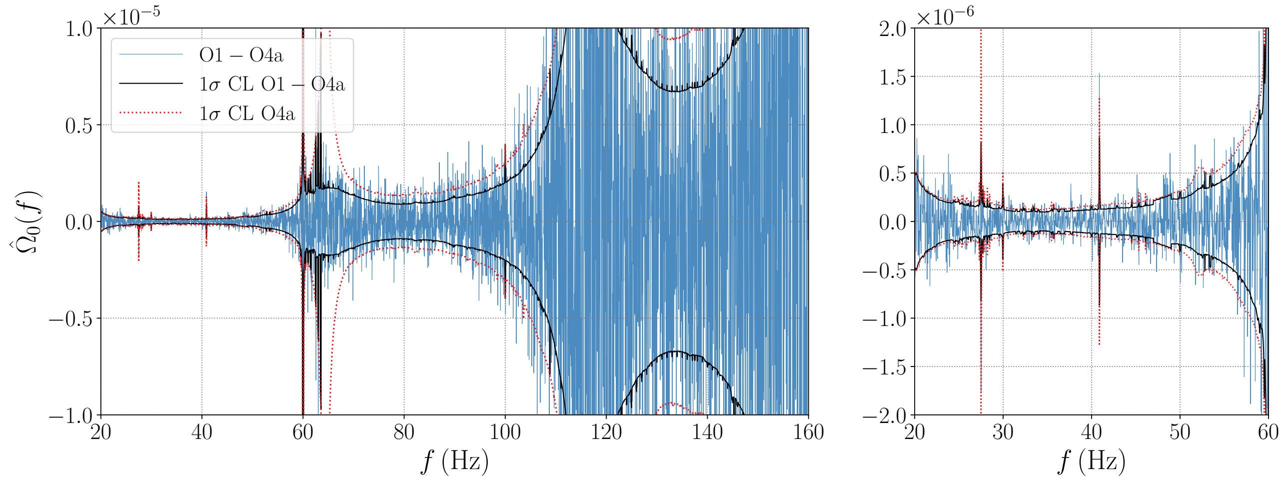

FIG. 2. Cross-correlation spectrum obtained from O1 to O4a data. The black lines denote the boundaries of the 1σ region: the dotted line shows results calculated from O4a data, while the solid line corresponds to the full O1−O4a dataset. The spectrum remains consistent with 0 across all frequency bins, indicating no evidence of a signal. The left panel shows the spectrum over the 20−160 Hz range, while the right panel zooms in on frequencies below 60 Hz to highlight the contribution from O4a data at these frequencies.

Power law	$f_{99\%}^{\rm O4a}$[Hz]	$\hat{\Omega}^{\rm O4a}/10^{-9}$	$f_{99\%}^{\rm O1-O4a}$ [Hz]	$\hat{\Omega}^{\rm O1-O4a}/10^{-9}$
0	54.8	-2.2 ± 5.8	58.2	-1.3 ± 4.7
2/3	83.6	-1.6 ± 4.5	86.8	-1.2 ± 3.5
3	376.7	-0.1 ± 0.8	336.6	-0.3 ± 0.6

TABLE II. Search results for an isotropic GWB using cross-correlation optimal filtering for power-law GWBs with $\alpha = 0, 2/3, 3$. For each case, we report the point estimate and associated 1σ uncertainty of the amplitude $\hat{\Omega}_\alpha$ at 25 Hz, along with the frequency range from 20 Hz to $f_{99\%}$, which contains 99% of the total sensitivity. These estimates are derived by combining the individual values from independent frequency bins following Eq. (11). The final two columns show results obtained by combining data from all observing runs (O1−O4a) following the prescription shown in [74] (Eq. (7)). Note that Virgo data contributed to the O3 measurements, implying three separate baseline contributions to the O3 results.

- $\alpha = 2/3$ characterizes the CBC GWB when the inspiral phase dominates, which is a good approximation in the LVK frequency band [161]. However, this approximation may break down for mergers of binaries originating from Population III stars [162] or for heavy BBH mergers with masses exceeding the pair-instability mass gap [163].

- $\alpha = 3$ is a fiducial choice which provides an approximate description of a subset of astrophysical sources, such as supernovae [8, 164]. It also corresponds to a GWB with a flat strain power spectral density, following $S_h(f) \propto f^{-3}\Omega_{\rm GW}(f)$ [108]. This is the spectral shape detectors are most sensitive to by construction, as the optimal filter depends solely on the noise PSD, hence frequencies are weighted according to the detector sensitivity thereby maximizing the cross-correlation search sensitivity.

The point estimate spectrum $\hat{\Omega}_0(f)$ computed as defined in Eq. (7) is shown in Fig. 2. The 1σ contours calculated from O4a data as well as the entire O1−O4a dataset are compatible with 0, as expected in the presence of uncorrelated noise and in the absence of a correlated gravitational-wave signal. This behavior is consistent with the expectation that, after applying the data quality cuts described in Section III, the data remain dominated by Gaussian noise. This is further demonstrated by the Kolmogorov-Smirnov (KS) test, which returns a p-value of $p = 0.99$ in favour of Gaussianity.

Point estimates $\hat{\Omega}_\alpha$ and 1σ uncertainty using the O4a data only as well as combined results from all the advanced observing runs are presented in Table II. Point estimates for all spectral models are consistent with 0 within 1σ, which implies no detection of a GWB. We also report the upper edge of the frequency band that contributes 99% of the sensitivity to each spectral-weighted search, $f_{99\%}$.

We observe a decrease in variance with increasing spectral index, which is expected since, as mentioned above, our search is most sensitive to a flat strain spectrum ($\alpha = 3$). Notably, the sensitivity improvement compared to O1−O3 results is a factor of 1.6 for $\alpha = 0$, 1.6 for $\alpha = 2/3$, and 1.4 for $\alpha = 3$. This is driven by the fact that the most significant sensitivity enhancement in our detectors occurred at lower frequencies [131], below 40 Hz, as discussed below.

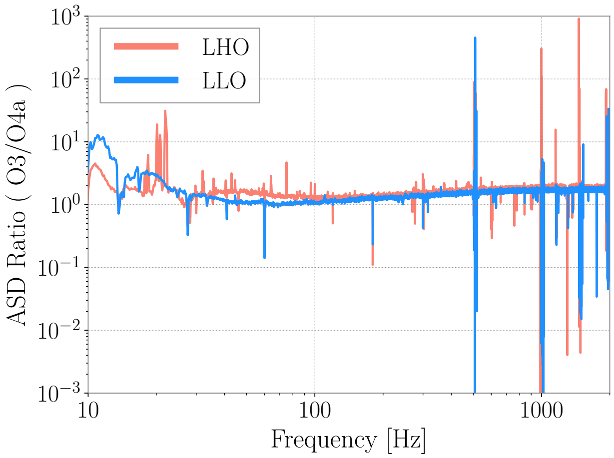

FIG. 3. Ratio of the detector strain sensitivity curves between O3 and O4a for LHO (blue) and LLO (red). A ratio above unity indicates an improvement in sensitivity compared to O3.

Altogether, these observations indicate that there is no evidence for a detectable GWB in the analyzed data. We also note that O4a contributes primarily at frequencies below 60 Hz, as highlighted in the right-hand-side panel of Fig. 2 which shows the portion of the spectrum in the $20-60$ Hz band, where the 1σ contours from O4a and O1−O4a data are almost overlapping. The frequency dependence of the sensitivity change between O4a and O3 is described in Fig. 3, which shows the ratio of the PSDs calculated in the two runs. We observe that this ratio lies consistently above 1 in the range $10-60$ Hz, which matches the range highlighted in Fig. 3 where the O4a data contributes the most to the measurement of a stochastic spectrum. The effect of this frequency-dependent improvement in sensitivity to the GWB between O4a and past runs is further quantified below.

B. Upper Limits on the GWB

Given the absence of evidence for a signal (see Table II), we set upper limits on the amplitude of the GWB, assuming a power-law model as in Eq. (5). The narrow-band estimators $\hat{\Omega}_0(f)$ and $\sigma_0(f)$ are employed in inference as described in Sec. II B, where the frequency lines described in Sec. III E are notched from the spectra. We explore different priors for both the amplitude and the spectral index. Specifically, we consider uniform and log-uniform priors for the amplitude, and uniform and Gaussian priors on the spectral index. A log-uniform prior is more sensitive to signals of small amplitude, yielding tighter constraints, while a uniform prior provides more conservative limits. In both cases, we set the prior range for the $\Omega_{\rm ref}$ parameter between $\Omega_{\rm ref,min} = 10^{-13}$ and $\Omega_{\rm ref,max} = 10^{-6}$.

We perform a fixed model analysis, fixing the spectral index to $\{0, 2/3, 3\}$, where each value corresponds to a specific source as indicated above. We also perform joint inference on the amplitude and spectral index, where we test both a Gaussian prior and uniform prior on the latter. The uniform prior range is set to $\alpha \in [-7, 7]$ [5]. In the case of a Gaussian prior on α, we impose zero mean and a standard deviation of

$$\frac{\log_{10}\Omega_{\rm ref,max} - \log_{10}\Omega_{\rm ref,min}}{2} = 3.5. \quad (17)$$

The choice of the prior over α can be understood as follows. The log-uniform prior over $\Omega_{\rm ref}$ induces some implicit prior over α that can be shown [113] to be a triangular prior centered on $\alpha = 0$ and non-zero for $|\alpha| \le (\log_{10}\Omega_{\rm ref,max} - \log_{10}\Omega_{\rm ref,min})$. To avoid a vanishing prior outside of this range, we choose a Gaussian prior for α with a standard deviation comparable with the triangular prior [113].

We set spectral-independent constraints on the signal amplitude by marginalizing over the spectral index posteriors obtained with the Gaussian prior. We take the results obtained with the log-uniform prior on the amplitude as our main result.

Table III summarizes results for the fixed spectral index and marginalized analyses. We set 95% confidence level upper limits on $\Omega_{\rm ref}$ at $f_{\rm ref} = 25$ Hz at individual values of α, $\Omega_{\rm ref}^{(\alpha)}$, fixing the α prior to a delta function at the chosen values; we also set upper limits marginalized over the Gaussian α posterior. For comparison, we report the corresponding upper limits from O1−O3 analyses. As expected, log-uniform priors on the background amplitude yield tighter constraints compared to uniform priors. Broadband constraints at 25 Hz are tightest for $\alpha = 3$ as this corresponds to a flat strain power spectrum, yielding the most broadband detectable signal, while constraints are weakest for a scale-invariant spectrum as this signal corresponds to a strain power spectrum with the most negative spectral index out of the set. Furthermore, marginalized results over the spectral index yield overall weaker constraints as these admit higher uncertainty on the signal model. Overall, we observe improvements in the upper limits ranging from a factor of 1.2 to 2.3.

Posterior distributions for $\Omega_{\rm ref}$ and α obtained in these analyses are shown in Fig. 4 assuming a log-uniform prior on $\Omega_{\rm ref}$ and either a Gaussian or uniform prior on α. As may be observed in Fig. 4, α is not constrained, and the prior on α has little impact on the $\Omega_{\rm ref}$ posteriors. The Bayes factor comparing the signal-versus-noise hypothesis to the noise-only hypothesis is $\log_{10}\mathcal{B} = -0.19 \pm 0.03$ ($\log_{10}\mathcal{B} = -0.11 \pm 0.03$) at 68% confidence level assuming a Gaussian (uniform) prior on α, further confirming no evidence of a signal in the data.

[5] This prior has been widened with respect to past analyses [74], which employed $\alpha \in [-5, 5]$, to investigate a small mode in the posterior in α which appeared at the edge of the prior range, as discussed below.

	Uniform prior			Log-uniform prior		
α	O1-O4a	O1-O3	Improvement	O1-O4a	O1-O3	Improvement
0	8.6×10^{-9}	1.7×10^{-8}	2.0	2.8×10^{-9}	5.8×10^{-9}	2.1
2/3	6.3×10^{-9}	1.2×10^{-8}	1.9	2.0×10^{-9}	3.4×10^{-9}	1.7
3	1.0×10^{-9}	1.3×10^{-9}	1.3	3.2×10^{-10}	3.9×10^{-10}	1.2
Marginalized	1.5×10^{-8}	2.7×10^{-8}	1.8	2.9×10^{-9}	6.6×10^{-9}	2.3

TABLE III. Upper limits at 95% CL on the amplitude $\Omega_{\rm ref}$ of the GWB assuming uniform (left) and log-uniform (right) prior. We quote the upper limits obtained employing data up to the O4a data run (O1−O4a), comparing these with those obtained previously [74] (O1−O3), at individual values of α (which corresponds to imposing a delta function prior on α at the quoted value), and marginalized over the α posterior (assuming a Gaussian prior on α). We observe an overall improvement between a factor 1.2 to 2.3. The improvement in upper limits compared to O3 is more significant for smaller spectral indices. This is because the greatest enhancement in detector sensitivity occurred at low frequencies. Furthermore, the difference between the upper limit for $\alpha = 0$ and the marginalized case is minimal, due to statistical fluctuations from the MCMC.

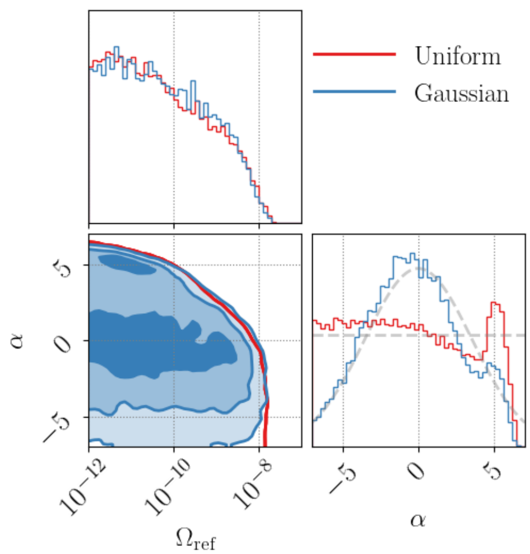

FIG. 4. Posterior distributions on the power-law model parameters $\{\Omega_{\rm ref}, \alpha\}$ obtained assuming a log-uniform prior on $\Omega_{\rm ref}$ and either a Gaussian (blue) or a uniform (red) prior on α. Prior functions for the α parameter are included in the corresponding one-dimensional panel (gray dashed lines).

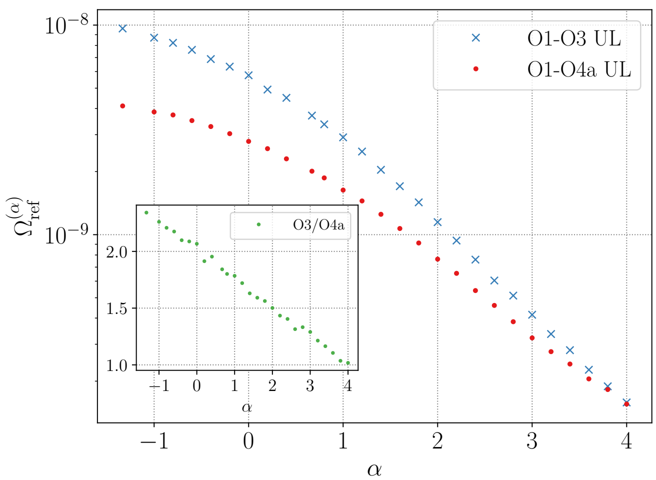

FIG. 5. Upper limits (UL) on $\Omega_{\rm ref}^{(\alpha)}$ at 95% CL as a function of α, obtained assuming the GWB is described by a power-law model using a log-uniform prior on the amplitude $\Omega_{\rm ref}^{(\alpha)}$. The blue curve shows the results using data from O1 to O3, while the red curve includes O4a data as well. The inset plot shows the ratio between the two sets of limits, highlighting improvement in O4a as a function of spectral weighting.

We point out a small narrow mode that appears in the posterior plot at $\alpha = 5$, present for both prior assumptions and more evident in the case of a uniform prior on α. Note that $\alpha = 5$ is not associated with any known physical GW signals and usually coincides with the edge of the broad prior range assumed for this analysis, however in this case the prior was broadened to confirm no railing was occurring. This mode has been traced back to weak, broad-band residual noise coherence between the LHO and LLO detectors during O4a in the $650 - 850\,$Hz band, which corresponds to the frequency range most sensitive to an $\alpha = 5$ power-law signal. The ORF introduced in Eq. (2) for the LHO–LLO baseline is highly suppressed at these frequencies (to $\sim 0.2 - 0.1\%$ relative to its magnitude at 1 Hz), strongly suggesting this weak coherence is detector noise and not GW signal. Excluding this frequency range from the analysis removes this feature completely. The four 60 Hz power-line harmonics in this range, [660, 720, 780, 840] Hz, appear significantly wider and noisier than in past observing runs, hence notches around these lines have been widened accordingly for this analysis. Numerous other weak unidentified noise features such as broadened lines and bumps have been found in both detectors. While these are not loud enough to significantly impact the analysis presented here, as demonstrated by broad-band signal point estimates (Table II) as well as the Bayes' factors above, the significance of this feature will be revisited in the next portion of the O4 data.

Finally, Fig. 5 shows upper limits on $\Omega_{\rm ref}$ at 95% CL as a function of α. Note that α values in this plot are not directly motivated by specific sources, but rather are chosen to highlight the overall trend: upper limits decrease as the spectral index increases, which is expected due to the extrapolation of the low-frequency sensitivity at higher frequencies, and as a consequence of $\Omega_{\rm GW} \propto f^3 S_h(f)$. Fig. 5 also includes upper limits obtained up to and including the O3 data run. The relative improvement between these and the limits obtained including O4a decreases as α increases, indicating that the sensitivity enhancement between runs is more significant at lower frequencies, as discussed above.

C. Non-GR polarizations

We employ the approach first presented in [113] to constrain potential deviations from GR. The detection of scalar or vector polarization modes would provide direct evidence of a violation of GR, whereas their absence allows us to place stringent constraints on extended theories of gravity.

Multiple runs with differently polarized backgrounds were conducted. First, we consider a mixed-polarized background, as introduced in Sec. II C. In this scenario, the parameters of our model are

$$\Theta = \{\Omega_{\rm ref,T}, \Omega_{\rm ref,V}, \Omega_{\rm ref,S}, \alpha_{\rm T}, \alpha_{\rm V}, \alpha_{\rm S}\}\,. \tag{18}$$

We set a log-uniform prior on the amplitudes $\Omega_{\rm ref,(p)}$, for (p) $= \{\rm T, V, S\}$, over the range 10^{-13} to 10^{-6} and a Gaussian prior on the spectral indices, centered at 0 with a standard deviation of 3.5. We set 95% CL upper limits on $\Omega_{\rm ref,(p)}$, presented in the third column of Table IV. We find an improvement in the upper limits of over a factor of 2 with respect to O3 results [74]. It is worth noting that the upper limit for the scalar-polarized case is less stringent as the ORF for scalar polarization is approximately three times smaller in amplitude than those for other polarizations [113]. As a result, our detector network is inherently less sensitive to a scalar-polarized background.

Polarization	**O1−O3**	**O1−O4a**	**Improvement**
Tensor	$6.4 \cdot 10^{-9}$	$2.6 \cdot 10^{-9}$	~ 2.5
Vector	$7.9 \cdot 10^{-9}$	$2.9 \cdot 10^{-9}$	~ 2.7
Scalar	$2.1 \cdot 10^{-8}$	$7.4 \cdot 10^{-9}$	~ 2.8

TABLE IV. Upper limits (ULs) at 95% confidence level (CL) on the amplitude of each individual polarization assuming a mixed-polarized background. The are improved by over a factor of 2 compared to ULs obtained from O1−O3 data [74]. We observe the UL for the scalar-polarized case is less stringent as the ORF for scalar polarization is smaller in amplitude than those for other polarizations [113].

Additionally, we set upper limits on the amplitudes $\Omega_{\rm ref,T}(25{\rm Hz}) \le 2.9 \cdot 10^{-9}$, $\Omega_{\rm ref,V}(25{\rm Hz}) \le 2.7 \cdot 10^{-9}$ and $\Omega_{\rm ref,S}(25{\rm Hz}) \le 2.9 \cdot 10^{-9}$, assuming single-polarized backgrounds. The upper limits are similar across polarizations due to the reduced detector network in O4a, since only LHO and LLO were operational, unlike O3 which included all three detectors. This limits our ability to distinguish polarization modes.

The signal versus noise hypothesis Bayes factor yields $\log_{10}\mathcal{B} = -0.87 \pm 0.01$ at 68% confidence level, indicating no evidence for the presence of a signal in our data. In this case, the signal is defined as the equal-weighted combination of the individual polarization components, $\{\rm T, V, S\}$, as well as their combinations: tensorvector (TV), tensorscalar (TS), vectorscalar (VS), and tensorvectorscalar (TVS). This approach treats all signal configurations equally.

Additionally, the Bayes factor for non-GR versus GR-supported polarized backgrounds yields $\log_{10}\mathcal{B} = -0.44 \pm 0.03$ at 68% confidence level. This result suggests that a tensor-polarized background (in accordance with GR) is favoured over vector, scalar, and mixed-polarized alternatives. However, in the absence of a detection we expect this result to be driven by the Occam penalty factor introduced by overfitting un-informed parameters in the search.

D. Joint fit for GWB and magnetic noise

Correlated magnetic noise can provide a significant limitation to the search for an isotropic stochastic signal [112, 144–146]. To mitigate this, the likelihood presented in Eq. (12) may be extended to jointly model correlated magnetic noise appearing in the GW detectors and a GWB power-law signal, as described in [165]:

$$\Omega_{\rm GW}(f|\Theta) = \Omega_{\rm ref} F_\alpha(f) + \Omega_{\rm MAG}(f|\Theta_{\rm MAG})\,. \tag{19}$$

In Section III F, we showed that correlated magnetic noise is not expected to contaminate O4a data. Nevertheless, this analysis provides a complementary check by simultaneously fitting both the GWB and the correlated magnetic noise. Instead of utilizing the measured coupling functions at the detectors from Section III F, we now model the magnetic term $\Omega_{\rm MAG}$ with the parameters $\Theta_{\rm MAG} = \{\kappa_I, \kappa_J, \beta_I, \beta_J\}$, approximating the inside-to-strain magnetic coupling functions $T_{I,\rm ITS}(f)$ as a simple power law,

$$|T_{I,\rm ITS}(f)| = \kappa_I \left(\frac{f}{10{\rm Hz}}\right)^{-\beta_I}, \tag{20}$$

where κ_I is the magnitude of the amplitude at 10 Hz and β_I is the spectral index of the power law. The prior distribution for κ_I is log-uniform in the range 10^{-25} to $10^{-22}\,{\rm pT}^{-1}$ for both detectors and the prior on the spectral index β_I is uniform in the range $0-12$ and $1-10$ for HLO and LLO respectively, related to measured minimum and maximum values of the spectral index during magnetic injections. As before, the GWB model parameters are $\Omega_{\rm ref}$ and α. This allows us to estimate either the evidence for a simultaneous measurement of a background and correlated magnetic noise, or estimate the evidence for correlated magnetic noise only.

We set joint constraints on the power-law GWB and the magnetic correlated noise, employing the same priors for the magnetic parameters as in the O3 analysis [74]. We find the log Bayes factor comparing a magnetic noise model to a (Gaussian) noise-only model is $\log_{10} \mathcal{B}_N^{\rm MAG} = -0.048$, indicating no evidence in favour of the presence of magnetic noise. We also find that for a joint model with a power-law background and magnetic noise modeled as described above that $\log_{10} \mathcal{B}_N^{\rm PL+MAG} = -0.306$, showing no preference for such a model compared to a noise-only model.

V. ASTROPHYSICAL IMPLICATIONS

Leveraging the upper limits on the GWB presented in Section IV B, we examine the implications of these results for the GWB of astrophysical origin, namely from the coalescing population of compact binaries including BBHs, BNSs, and NSBHs. We compare our upper limits to the most recent predictions for the energy density spectrum associated with different classes of CBC sources. In particular for BBHs, following Ref. [76], we combine BBH observations in the local Universe with stochastic upper limits to constrain their merger rate at high redshifts, and predict the uncertainty in the BBH background using a fully GW data-driven approach.

A. CBC Model

To model the GWB from binary systems we follow in part the approach of LVK isotropic search papers from the O1 to O3 observing runs [74, 106, 107, 166], and additionally we introduce advances in our knowledge of the CBC population [89, 167, 168]. We categorize the population into classes, each labeled by k, to differentiate between BBHs, BNSs and NSBHs. Each class is characterized by distinct values of source parameters, such as masses and spins, which we denote as θ_k. The total astrophysical background is then the sum of contributions from all classes. The contribution of class k to the background can be expressed as an integral over the redshift z, given by [82, 169–171]

$$\Omega_{\rm GW}(f;\theta_k) = \frac{f}{\rho_c H_0} \int_0^{z_{\rm max}} dz \frac{R_m(z;\theta_k)\langle \frac{dE_{\rm GW}}{df_s}(f_s;\theta_k)\rangle}{(1+z)E(\Omega_{\rm m,0},\Omega_{\Lambda,0},z)}, \tag{21}$$

where $R_m(z;\theta_k)$ denotes the binary merger rate in the source frame per unit comoving volume, $\langle dE_{\rm GW}/df_s(f_s,\theta_k)\rangle$ is the energy spectrum emitted by a single binary evaluated in terms of the source frequency $f_s = (1+z)f$ and averaged over the ensemble properties of source class k, and $E(\Omega_{\rm m,0},\Omega_{\Lambda,0},z) = \sqrt{\Omega_{\rm m,0}(1+z)^3+\Omega_{\Lambda,0}}$ accounts for the dependence of comoving volume on cosmology, assuming $\Omega_{\Lambda,0} = 1-\Omega_{\rm m,0}$. We impose an upper redshift cutoff at $z_{\rm max} = 10$, beyond which the compact binary merger rate in conventional formation scenarios is expected to be negligible [172]. We do not consider potential contributions to the GWB from formation channels involving Population III stars [173] or primordial black holes [174, 175].

The energy spectrum $\langle dE_{\rm GW}/df_s\rangle$ is determined from the strain waveform of the binary system. For computing the backgrounds of BBH and NSBH we use `IMRPhenomXP`, a phenomenological inspiral-merger-ringdown frequency-domain model for gravitational-wave signals emitted by quasi-circular precessing BBHs [176, 177]. For BNS background computation, we employ the `IMRPhenomXP_NRTidalv3` waveform model, which tapers the merger-ringdown part from the baseline `IMRPhenomXP` model and has the option to include tidal effects [178–180]. To compute the GWB from CBCs throughout the Universe according to Eq. (21), we use methods developed for the GWB calculation in [74, 84], as well as `popstock`, a Python-based module that predicts the background spectrum and its uncertainty given a CBC population and merger rate evolution [83].

B. Binary black holes

To model the BBH background we generally follow the approach in [74] with some adjustments in the presumed mass, redshift, and spin distributions of BBHs.

In [74] it was assumed that the BBH primary mass distribution is approximated by a mixture between a Gaussian peak near 35 $M_\odot$ and a power-law continuum, that mass ratios are power-law distributed, and, for simplicity, that spins are negligible. We update these assumptions to match the latest understanding of the black hole population in GWTC-4 [88]. Following [89], we assume that black hole primary masses follow a mixture between two Gaussians, centered near 10 $M_\odot$ and 35 $M_\odot$, and a broken power-law continuum extending up to 200 $M_\odot$. Whereas we previously neglected spins, we now include a realistic model for the black hole spin distribution; we follow [89] and assume spin magnitudes are described by a truncated normal distribution and spin orientations by a mixture between isotropic and preferentially-oriented subpopulations. Black hole mass ratios are again assumed to be power-law distributed. As in [74], we do not fix the parameters of these models, but instead show a projection for $\Omega_{\rm BBH}(f)$ that self-consistently includes observational uncertainties in the BBH mass, spin, and mass ratio distributions.

Previous forecasts of the BBH background included uncertainties in the ensemble of intrinsic black hole properties and the local BBH merger rate, while imposing a *fixed* fiducial model describing how this rate evolved with redshift. In [74], for example, we assumed a BBH birth rate proportional to low-metallicity star formation, with a power-law time delay distribution between binary formation and merger. Here, we revise our projections to additionally reflect systematic uncertainties in the BBH merger rate. We assume the BBH merger rate density follows the broken power law [181]

$$R_{\rm BBH}(z) = C(\alpha_z, \beta_z, z_{\rm p}) \frac{R_0(1+z)^{\alpha_z}}{1+\left(\frac{1+z}{1+z_{\rm p}}\right)^{\alpha_z+\beta_z}}, \quad (22)$$

where parameters α_z and β_z represent the low and high redshift power laws to which the merger rate history asymptotes, respectively, while $z_{\rm p}$ is the redshift at which the merger rate history peaks. Specifically, Eq. (22) implies that $R_{\rm BBH}(z) \propto (1+z)^{\alpha_z}$ for redshifts $z \ll z_{\rm p}$ and $R_{\rm BBH}(z) \propto (1+z)^{-\beta_z}$ for $z \gg z_{\rm p}$, and the normalization constant $C(\alpha_z, \beta_z, z_{\rm p})$ is defined such that $R_{\rm BBH}(z) = R_0$ at $z = 0$. This parametrization allows us to cover a broad range of theoretical predictions for the redshift evolution of the BBH merger rate. It accommodates scenarios involving isolated binary evolution, where the merger rate closely follows the metallicity-dependent cosmic star formation rate with a distribution of time delays between formation and merger [182–184]. At the same time, it can represent dynamically assembled mergers in dense star clusters, which are less directly tied to star formation and often exhibit a merger rate that peaks at higher redshifts [185, 186].

We combine all direct detections of BBHs in GWTC-4 with our updated constraints on the astrophysical GWB to measure the underlying distributions of BBH primary masses, mass ratios, spins, and redshifts. We assume these distributions are well-described by the models listed above, and we follow the methods presented in [76–78, 89]. In order to self-consistently combine data from direct BBH detections with constraints on the GWB, we adopt a factorized likelihood given by

$$p(\hat{\Omega}_0, \{d_i\}|\Lambda_{\rm BBH}) = p_{\rm BBH}(\{d_i\}|\Lambda_{\rm BBH}) \times p_{\rm stoch}(\hat{\Omega}_0|\Lambda_{\rm BBH}) \, . \quad (23)$$

Here, $p_{\rm stoch}(\hat{\Omega}_0|\Lambda_{\rm BBH})$ is the likelihood of our cross-correlation measurements [see Eq. (12)], given a BBH population model denoted $\Lambda_{\rm BBH}$. Meanwhile, $p_{\rm BBH}(\{d_i\}|\Lambda_{\rm BBH})$ is the likelihood of the direct compact binary detections comprising GWTC-4 [89]. In practice, rather than evaluating Eq. (23) directly, we sample the likelihood in a two step process, first sampling from the posterior $p_{\Lambda_{\rm BBH}|{\rm BBH}}(\{d_i\})$ and then rejection sampling these draws using $p_{\rm stoch}(\hat{\Omega}_0|\Lambda_{\rm BBH})$. The resulting $\Omega_{\rm BBH}(f)$ spectra calculated from each posterior sample Λ after rejection sampling are shown in the left-hand side of Fig. 6. At a reference frequency of 25 Hz, we predict $\Omega_{\rm BBH}(25\,{\rm Hz}) = 0.8^{+1.3}_{-0.5} \times 10^{-9}$ before rejecting according to the GWB upper limits. After rejection sampling, the predicted BBH GWB amplitude is $\Omega_{\rm BBH}(25\,{\rm Hz}) = 0.8^{+1.1}_{-0.5} \times 10^{-9}$. Here and henceforth, all uncertainties are quoted as 90% credible intervals.

The inferred BBH merger rate $R_{\rm BBH}(z)$ is shown in the right side of Fig. 6. Black and red curves again show 90% credible bounds and individual posterior samples, respectively. The present-day merger rate is inferred to be $R_0 = 15.4^{+6.0}_{-4.5}\,{\rm Gpc^{-3}\,yr^{-1}}$. For comparison, dotted black curves indicate 90% credible bounds obtained previously when analyzing BBH mergers in GWTC-3 [168, 188]. New results are consistent with previous estimates, although it is now found that the rate with which $R_{\rm BBH}(z)$ increases ($\alpha_z = 3.2^{+1.1}_{-1.0}$) is near the upper end of previous bounds ($\alpha_z = 2.7^{+2.2}_{-1.9}$). The high redshift parameters β_z and $z_{\rm p}$ remain poorly constrained ($\beta_z = 5.1^{+4.5}_{-4.6}$, $z_{\rm p} = 2.6^{+1.2}_{-1.3}$).

The forecasted $\Omega_{\rm BBH}(25\,{\rm Hz})$ reported above is approximately a factor of two larger than previously estimated in [74] and [168]. This increase is due primarily to two effects. The increased sample of direct compact binary detections indicates that the BBH merger rate likely increases more quickly with redshift than previously measured. Secondly, whereas past forecasts used simple parametric estimates for the energy spectrum of a given binary [189], our updated forecasts adopt the significantly more mature `IMRPhenomXP` waveform model to compute radiated energy.

The non-detection of a stochastic background provides an additional constraint on the population history of BBHs, effectively ruling out scenarios with high merger rates at large redshifts that would otherwise yield a detectable background signal [76]. While the background upper limits effectively do not impact the inferred merger rate, these imply a modest tightening of the upper uncertainty bound on the BBH background amplitude as described above. This result implies that, when modeling the BBH merger history via Eq. (22), the direct detections already require α_z to be sufficiently small that most possible astrophysical backgrounds lie below the current detection threshold. In future observing runs, the exact degree to which stochastic search results are or are not informative will depend on the achieved sensitivity and run duration, as well as updated inference of α_z.

C. Binary neutron stars

Since neither the local merger rate nor the mass and spin distribution of BNS mergers are well constrained from current GW catalogs, we cannot adopt detailed data-driven models of the BNS population. Instead, we forecast the astrophysical background from BNSs using the methodology of [74], which adopts a fixed star formation history convoluted with a time delay distribution and simplified assumptions for mass and spin. We assume that BNS progenitor formation follows the star formation rate described in [190] (Eq.(22) with $\alpha_z = 2.6$, $\beta_z = 3.6$ and $z_p = 2.2$), with a distribution $p(t_d) \sim t_d^{-1}$ of time delays t_d between binary formation and merger, where 20 Myr $< t_d <$ 13.5 Gyr. Following [89], we assume a simple fixed population model, with a uniform mass distribution between $1 - 2.5\,M_\odot$ and isotropic spin orientations with uniformly distributed spin magnitudes below 0.4. Under these assumptions, the local merger

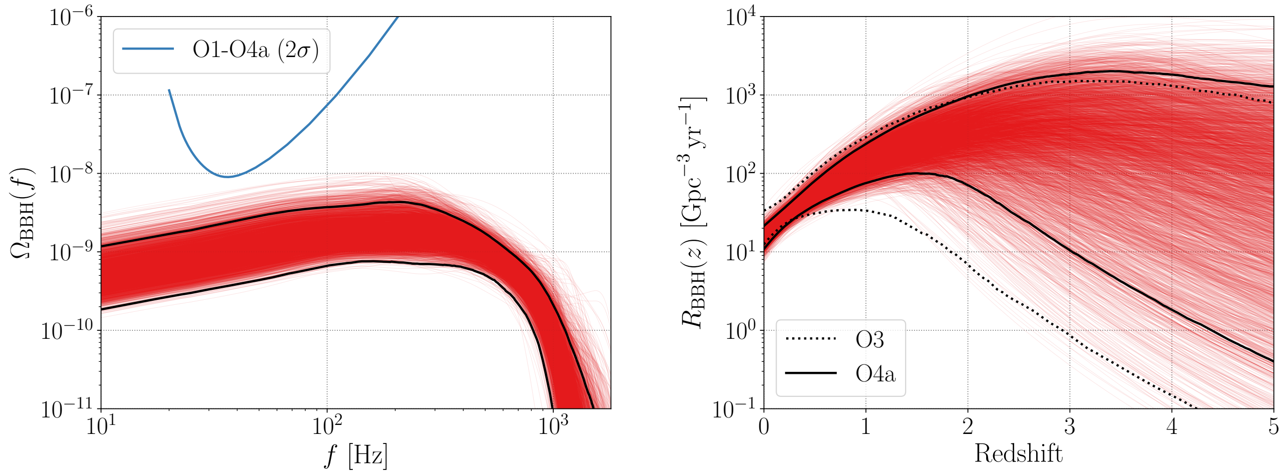

FIG. 6. *Left:* Forecast for the stochastic energy-density spectrum of the BBH population, given the population of direct BBH detections within the LVK GWTC-4 catalog [89] and the GWB upper limit presented here. The black curves indicate 90% credible bounds on $\Omega_{\rm BBH}(f)$, while red traces show individual posterior samples on the energy-density spectrum, obtained by sampling over the possible mass, spin, and redshift distributions of BBH mergers. For comparison, the blue curve indicates the 2σ PI curve calculated using O1−O4a HLV data [150], integrated over all observing runs to date. *Right:* Inferred redshift evolution of the BBH merger rate density, measured hierarchically using the direct BBH detections in GWTC-4 and the GWB upper limit. Solid black and red lines again mark 90% credible bounds and individual posterior samples, respectively, while dotted black lines denote the 90% credible bounds obtained previously with GWTC-3 [168].

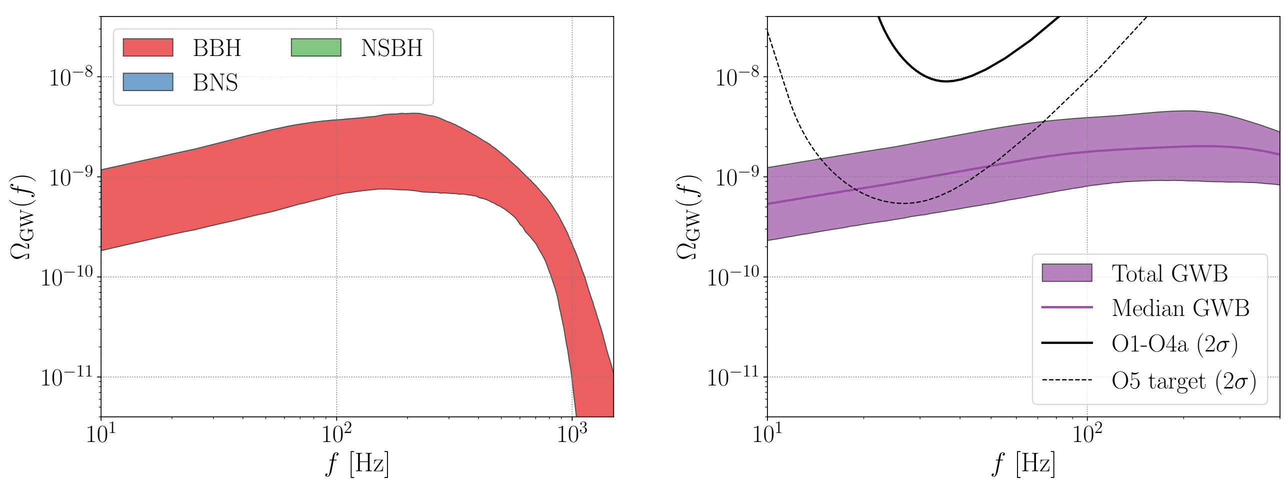

FIG. 7. *Left:* Projected astrophysical GWB contributions from BBH, BNS and NSBH coalescences. Shaded bands represent the 90% credible bounds for each CBC class. *Right:* The solid purple line shows the median estimate of $\Omega_{\rm BBH+BNS+NSBH}(f)$ as a function of frequency, while the shaded purple band illustrates 90% credible uncertainties. We also show the 2σ PI sensitivity curve calculated using data from stochastic isotropic searches O1 through O4a, considering the three HLV baselines. We include the target 2σ PI curve for O5, assuming the target sensitivity curves for the HLV baselines as detailed in [187] and [91] .

rate is estimated to be 61^{+113}_{-48} Gpc^{-3}yr^{-1}. When modeling $\Omega_{\rm BNS}(f)$, we do not consider any tidal effects nor contributions from a potential post-merger signal [191]. These modeling choices lead to an estimated BNS GWB shown in Fig. 7, specifically at the reference frequency of 25 Hz, we predict $\Omega_{\rm BNS}(25{\rm Hz}) = 3.6^{+6.7}_{-2.8} \times 10^{-11}$.

D. Neutron star-black hole binaries

Similar to BNSs, few compact binaries with masses consistent with NSBH systems have been observed [192–194], and so the details of the NSBH population remain largely unknown. As in the BNS case above, we again follow the simplified modeling approach undertaken previously in [168]. The black hole masses are drawn from a log-uniform distribution between 3 and 50 $M_\odot$, and neutron star masses from a uniform distribution between $1-2.5\,M_\odot$. Black hole spins are assumed to be isotropically distributed with uniform spin magnitude below 0.99, while the neutron star spin follows the same distribution as for BNS. The energy emission from NSBH binaries is calculated using the BBH waveform model `IMRPhenomXP`, which provides a reliable approximation, especially for systems with large mass ratios [195]. However, the model does not include tidal deformability or the possibility of tidal disruption of the neutron star, effects that can affect the emitted GW signal from binaries with more comparable component masses [196]. For the given population model, the local merger rate of NSBH binaries is estimated to be 30^{+34}_{-19} $\mathrm{Gpc^{-3}yr^{-1}}$ [89]. Moreover, we assume that the rate evolves in redshift in a manner identical to BNS systems as described above.

With these assumptions we find $\Omega_{\rm NSBH}(25\mathrm{Hz}) = 5.0^{+5.6}_{-3.1}\times 10^{-11}$. The 90% credible band over the whole frequency range is displayed in Fig. 7. We note that $\Omega_{\rm NSBH}(f)$ is predicted to be significantly flatter than in past estimates, deviating noticeably from a canonical $f^{2/3}$ power law above $\sim 30\,\mathrm{Hz}$. This change is primarily due to our adoption of an updated waveform model, in which the energy spectra of highly unequal-mass binaries are suppressed at high frequencies.

E. Total compact binary background

In Fig. 7 (right hand side), we present an updated estimate of the combined CBC GWB. Our model predicts this background at $\Omega_{\rm BBH+BNS+NSBH}(25\mathrm{Hz}) = 0.9^{+1.1}_{-0.5}\times 10^{-9}$. Additionally, we show the estimated sensitivity of the search described in this paper by presenting the 2σ power-law integrated sensitivity curve including data from O1−O4a. Although our estimate for the background amplitude is below current limits, it may become accessible with the A+ configuration of the LIGO detectors. This may be seen from the comparison shown in Fig. 7 with the target 2σ power-law integrated sensitivity curve for the O5 data run (dashed curve), which includes substantial planned updates for the LIGO sites [131, 187] and the Virgo detector [91], and assumes one year of uninterrupted data. It is important to note that these are *target* sensitivities that are expected to be reached by the end of the observing run, hence the O5 target sensitivity curve in Fig. 7 should be interpreted as an optimistic limit for the observing scenario.

VI. CONCLUSIONS

In this paper, we presented an isotropic search conducted on data spanning from the first LVK observing run (O1) to the first part of the fourth observing run (O4a), incorporating 115.51 days of new coincident LIGO-Hanford and LIGO-Livingston observation. No evidence for a GWB is found, and we limit the net energy density of the GWB to $\Omega_{\rm ref}(25\,\mathrm{Hz}) \leq 2.9\times 10^{-9}$ under a log-uniform prior ($\leq 1.5\times 10^{-8}$ under a uniform prior), an improvement of approximately a factor of 2 relative to previous bounds [74].

We additionally constrain alternative theories of gravity by searching for non-standard gravitational-wave polarizations, including scalar and vector modes beyond general relativity's tensor predictions. Our analysis improves existing bounds on these exotic polarization states by factors of two compared to previous datasets. However, the absence of any detectable background prevents us from distinguishing between standard tensor-only scenarios and models incorporating additional polarization modes.

As GWB searches improve in sensitivity, previously negligible terrestrial noise sources, including magnetic coupling from Schumann resonances and lightning activity, might contaminate our results and require characterization and possible mitigation. To quantify the potential impact of magnetic couplings on our result, we combine measurements of the magnetic environments surrounding LHO and LLO with measured transfer functions between external magnetic fields and measured strain, estimating a net magnetic noise budget. We find that, given current search sensitivities, contamination due to correlated magnetic environments does not significantly impact our results.

We conclude by examining how close our sensitivity has come to detecting the expected astrophysical background from the population of merging compact binaries across the Universe. We present updated estimates of energy-density spectra arising from distant binary black holes, binary neutron stars, and neutron-star black hole binaries, incorporating updated measurements of these sources' merger rates and demographics. Combining these three source classes, we estimate a total astrophysical background amplitude $\Omega_{\rm BBH+BNS+NSBH}(25\mathrm{Hz}) = 0.9^{+1.1}_{-0.5}\times 10^{-9}$, consistent with but marginally smaller than previous estimates [168]. This decrease is primarily driven by lower inferred BNS and NSBH merger rates, given the lack of such systems detected during O4a. This estimate lies at least a factor of three below the sensitivity of our search, and is thus consistent with a current non-detection of a GWB.

Several companion papers further extend the methodology presented here and elaborate on additional implications of a GWB non-detection. In this work, we have limited ourselves to exploring a purely isotropic stochastic background. Alternate analyses targeting anisotropic backgrounds are presented in [92]. Additionally, although we have commented on the astrophysical background expected from merging compact binaries, there exist a host of predicted mechanisms that may yield GWBs of cosmological origin. Implications of our updated constraints on the GWB on such cosmological backgrounds are discussed in [101].

VII. ACKNOWLEDGEMENTS

This material is based upon work supported by NSF's LIGO Laboratory, which is a major facility fully funded by the National Science Foundation. The authors also gratefully acknowledge the support of the Science and Technology Facilities Council (STFC) of the United Kingdom, the Max-Planck-Society (MPS), and the State of Niedersachsen/Germany for support of the construction of Advanced LIGO and construction and operation of the GEO 600 detector. Additional support for Advanced LIGO was provided by the Australian Research Council. The authors gratefully acknowledge the Italian Istituto Nazionale di Fisica Nucleare (INFN), the French Centre National de la Recherche Scientifique (CNRS) and the Netherlands Organization for Scientific Research (NWO) for the construction and operation of the Virgo detector and the creation and support of the EGO consortium. The authors also gratefully acknowledge research support from these agencies as well as by the Council of Scientific and Industrial Research of India, the Department of Science and Technology, India, the Science & Engineering Research Board (SERB), India, the Ministry of Human Resource Development, India, the Spanish Agencia Estatal de Investigación (AEI), the Spanish Ministerio de Ciencia, Innovación y Universidades, the European Union NextGenerationEU/PRTR (PRTR-C17.I1), the ICSC - CentroNazionale di Ricerca in High Performance Computing, Big Data and Quantum Computing, funded by the European Union NextGenerationEU, the Comunitat Autonòma de les Illes Balears through the Conselleria d'Educació i Universitats, the Conselleria d'Innovació, Universitats, Ciència i Societat Digital de la Generalitat Valenciana and the CERCA Programme Generalitat de Catalunya, Spain, the Polish National Agency for Academic Exchange, the National Science Centre of Poland and the European Union - European Regional Development Fund; the Foundation for Polish Science (FNP), the Polish Ministry of Science and Higher Education, the Swiss National Science Foundation (SNSF), the Russian Science Foundation, the European Commission, the European Social Funds (ESF), the European Regional Development Funds (ERDF), the Royal Society, the Scottish Funding Council, the Scottish Universities Physics Alliance, the Hungarian Scientific Research Fund (OTKA), the French Lyon Institute of Origins (LIO), the Belgian Fonds de la Recherche Scientifique (FRS-FNRS), Actions de Recherche Concertées (ARC) and Fonds Wetenschappelijk Onderzoek - Vlaanderen (FWO), Belgium, the Paris Île-de-France Region, the National Research, Development and Innovation Office of Hungary (NKFIH), the National Research Foundation of Korea, the Natural Sciences and Engineering Research Council of Canada (NSERC), the Canadian Foundation for Innovation (CFI), the Brazilian Ministry of Science, Technology, and Innovations, the International Center for Theoretical Physics South American Institute for Fundamental Research (ICTP-SAIFR), the Research Grants Council of Hong Kong, the National Natural Science Foundation of China (NSFC), the Israel Science Foundation (ISF), the US-Israel Binational Science Fund (BSF), the Leverhulme Trust, the Research Corporation, the National Science and Technology Council (NSTC), Taiwan, the United States Department of Energy, and the Kavli Foundation. The authors gratefully acknowledge the support of the NSF, STFC, INFN and CNRS for provision of computational resources. This work was supported by MEXT, the JSPS Leading-edge Research Infrastructure Program, JSPS Grant-in-Aid for Specially Promoted Research 26000005, JSPS Grant-in-Aid for Scientific Research on Innovative Areas 2402: 24103006, 24103005, and 2905: JP17H06358, JP17H06361 and JP17H06364, JSPS Core-to-Core Program A. Advanced Research Networks, JSPS Grants-in-Aid for Scientific Research (S) 17H06133 and 20H05639, JSPS Grant-in-Aid for Transformative Research Areas (A) 20A203: JP20H05854, the joint research program of the Institute for Cosmic Ray Research, University of Tokyo, the National Research Foundation (NRF), the Computing Infrastructure Project of the Global Science experimental Data hub Center (GSDC) at KISTI, the Korea Astronomy and Space Science Institute (KASI), the Ministry of Science and ICT (MSIT) in Korea, Academia Sinica (AS), the AS Grid Center (ASGC) and the National Science and Technology Council (NSTC) in Taiwan under grants including the Science Vanguard Research Program, the Advanced Technology Center (ATC) of NAOJ, and the Mechanical Engineering Center of KEK.

[1] J. Romano and N. Cornish, Living Reviews in Relativity **20** (2017), 10.1007/s41114-017-0004-1.

[2] N. J. Cornish and J. D. Romano, Phys. Rev. D **92**, 042001 (2015).

[3] S. Marassi, R. Schneider, G. Corvino, V. Ferrari, and S. P. Zwart, Phys. Rev. D **84**, 124037 (2011).

[4] X.-J. Zhu, E. Howell, T. Regimbau, D. Blair, and Z.-H. Zhu, Astrophysical Journal **739** (2011), 10.1088/0004-637X/739/2/86.

[5] P. A. Rosado, Phys. Rev. D **84**, 084004 (2011).

[6] C. Wu, V. Mandic, and T. Regimbau, Phys. Rev. D **85**, 104024 (2012).

[7] X.-J. Zhu, E. Howell, D. Blair, and Z.-H. Zhu, Monthly Notices of the Royal Astronomical Society **431** (2012), 10.1093/mnras/stt207.

[8] P. Sandick, K. A. Olive, F. Daigne, and E. Vangioni, Phys. Rev. D **73**, 104024 (2006).

[9] A. Buonanno, G. Sigl, G. G. Raffelt, H.-T. Janka, and E. Müller, Phys. Rev. D **72**, 084001 (2005).

[10] X.-J. Zhu, E. Howell, and D. Blair, Mon. Not. Roy. Astron. Soc. **409**, L132 (2010), arXiv:1008.0472 [gr-qc].

[11] V. Ferrari, S. Matarrese, and R. Schneider, Monthly Notices of the Royal Astronomical Society **303**, 258 (1999).
[12] P. D. Lasky, M. F. Bennett, and A. Melatos, Phys. Rev. D **87**, 063004 (2013).
[13] P. A. Rosado, Phys. Rev. D **86**, 104007 (2012).
[14] X.-J. Zhu, X.-L. Fan, and Z.-H. Zhu, Astrophys. J. **729**, 59 (2011), arXiv:1102.2786 [astro-ph.CO].
[15] K. Crocker, T. Prestegard, V. Mandic, T. Regimbau, K. Olive, and E. Vangioni, Phys. Rev. D **95**, 063015 (2017).
[16] K. Crocker, V. Mandic, T. Regimbau, K. Belczynski, W. Gladysz, K. Olive, T. Prestegard, and E. Vangioni, Physical Review D **92** (2015), 10.1103/PhysRevD.92.063005.
[17] R. Brito, V. Cardoso, and P. Pani, Lect. Notes Phys. **906**, pp.1 (2015), arXiv:1501.06570 [gr-qc].
[18] T. Takahashi, H. Omiya, and T. Tanaka, Phys. Rev. D **110**, 104038 (2024), arXiv:2408.08349 [gr-qc].
[19] M. Sasaki, T. Suyama, T. Tanaka, and S. Yokoyama, Phys. Rev. Lett. **117**, 061101 (2016).
[20] A. Arvanitaki and S. Dubovsky, Phys. Rev. D **83**, 044026 (2011).
[21] R. Brito, S. Ghosh, E. Barausse, E. Berti, V. Cardoso, I. Dvorkin, A. Klein, and P. Pani, Phys. Rev. Lett. **119**, 131101 (2017).
[22] T. W. B. Kibble, Journal of Physics A: Mathematical and General **9**, 1387 (1976).
[23] M. B. Hindmarsh and T. W. B. Kibble, Rep. Prog. Phys. **58**, 477 (1995), arXiv:hep-ph/9411342.
[24] T. Vachaspati, L. Pogosian, and D. Steer, Scholarpedia **10**, 31682 (2015), arXiv:1506.04039 [astro-ph.CO].
[25] K. Schmitz and T. Schrder, Physical Review D **110** (2024), 10.1103/PhysRevD.110.063549.
[26] B. P. Abbott, R. Abbott, T. D. Abbott, F. Acernese, K. Ackley, C. Adams, T. Adams, P. Addesso, R. X. Adhikari, *et al.* (LIGO Scientific Collaboration and Virgo Collaboration), Phys. Rev. D **97**, 102002 (2018).
[27] R. Abbott, T. D. Abbott, S. Abraham, F. Acernese, K. Ackley, A. Adams, C. Adams, R. X. Adhikari, V. B. Adya, and C. Affeldt (LIGO Scientific Collaboration, Virgo Collaboration, and KAGRA Collaboration), Phys. Rev. Lett. **126**, 241102 (2021).
[28] P. Auclair *et al.*, JCAP **04**, 034 (2020), arXiv:1909.00819 [astro-ph.CO].
[29] T. Damour and A. Vilenkin, Phys. Rev. Lett. **85**, 3761 (2000).
[30] T. Damour and A. Vilenkin, Phys. Rev. D **71**, 063510 (2005).
[31] X. Siemens, V. Mandic, and J. Creighton, Phys. Rev. Lett. **98**, 111101 (2007).
[32] S. Olmez, V. Mandic, and X. Siemens, Phys. Rev. D **81**, 104028 (2010), arXiv:1004.0890 [astro-ph.CO].
[33] T. Vachaspati and A. Vilenkin, Phys. Rev. D **31**, 3052 (1985).
[34] J. J. Blanco-Pillado and K. D. Olum, Phys. Rev. D **96**, 104046 (2017), arXiv:1709.02693 [astro-ph.CO].
[35] M. Kawasaki, K. Miyamoto, and K. Nakayama, Phys. Rev. D **81**, 103523 (2010), arXiv:1002.0652 [astro-ph.CO].
[36] E. Witten, Phys. Rev. D **30**, 272 (1984).
[37] C. J. Hogan, Mon. Not. Roy. Astron. Soc. **218**, 629 (1986).
[38] A. Mazumdar and G. White, Rept. Prog. Phys. **82**, 076901 (2019), arXiv:1811.01948 [hep-ph].
[39] M. B. Hindmarsh, M. Lüben, J. Lumma, and M. Pauly, SciPost Phys. Lect. Notes **24**, 1 (2021), arXiv:2008.09136 [astro-ph.CO].
[40] M. S. Turner and F. Wilczek, Phys. Rev. Lett. **65**, 3080 (1990).
[41] A. Kosowsky, M. S. Turner, and R. Watkins, Phys. Rev. D **45**, 4514 (1992).
[42] M. Kamionkowski, A. Kosowsky, and M. S. Turner, Phys. Rev. D **49**, 2837 (1994).
[43] A. Romero, K. Martinovic, T. A. Callister, H.-K. Guo, M. Martínez, M. Sakellariadou, F.-W. Yang, and Y. Zhao, Phys. Rev. Lett. **126**, 151301 (2021).
[44] C. Badger, B. Fornal, K. Martinovic, A. Romero, K. Turbang, H.-K. Guo, A. Mariotti, M. Sakellariadou, A. Sevrin, F.-W. Yang, and Y. Zhao, Phys. Rev. D **107**, 023511 (2023).
[45] B. J. Carr, Astrophys. J. **201**, 1 (1975).
[46] B. Carr, K. Kohri, Y. Sendouda, and J. Yokoyama, Rept. Prog. Phys. **84**, 116902 (2021), arXiv:2002.12778 [astro-ph.CO].
[47] S. Matarrese, S. Mollerach, and M. Bruni, Phys. Rev. D **58**, 043504 (1998), arXiv:astro-ph/9707278.
[48] D. Baumann, P. J. Steinhardt, K. Takahashi, and K. Ichiki, Phys. Rev. D **76**, 084019 (2007), arXiv:hep-th/0703290.
[49] K. Kohri and T. Terada, Phys. Rev. D **97**, 123532 (2018), arXiv:1804.08577 [gr-qc].
[50] A. Romero-Rodríguez, M. Martínez, O. Pujolàs, M. Sakellariadou, and V. Vaskonen, Phys. Rev. Lett. **128**, 051301 (2022).
[51] R. Inui, S. Jaraba, S. Kuroyanagi, and S. Yokoyama, Journal of Cosmology and Astroparticle Physics **2024** (2024), 10.1088/1475-7516/2024/05/082.
[52] T. Boybeyi, S. Clesse, S. Kuroyanagi, and M. Sakellariadou, Phys. Rev. D **112**, 023551 (2025).
[53] M. Giovannini, Phys. Rev. D **58**, 083504 (1998), arXiv:hep-ph/9806329.
[54] P. J. E. Peebles and A. Vilenkin, Phys. Rev. D **59**, 063505 (1999), arXiv:astro-ph/9810509.
[55] M. Giovannini, Phys. Rev. D **60**, 123511 (1999), arXiv:astro-ph/9903004.
[56] D. G. Figueroa and E. H. Tanin, JCAP **10**, 050 (2019), arXiv:1811.04093 [astro-ph.CO].
[57] D. G. Figueroa and E. H. Tanin, JCAP **08**, 011 (2019), arXiv:1905.11960 [astro-ph.CO].
[58] H. Duval, S. Kuroyanagi, A. Mariotti, A. Romero-Rodríguez, and M. Sakellariadou, Phys. Rev. D **110**, 103503 (2024).
[59] N. Barnaby, E. Pajer, and M. Peloso, Phys. Rev. D **85**, 023525 (2012), arXiv:1110.3327 [astro-ph.CO].
[60] N. Barnaby, R. Namba, and M. Peloso, JCAP **04**, 009 (2011), arXiv:1102.4333 [astro-ph.CO].
[61] A. Maleknejad, JHEP **07**, 104 (2016), arXiv:1604.03327 [hep-ph].
[62] B. Thorne, T. Fujita, M. Hazumi, N. Katayama, E. Komatsu, and M. Shiraishi, Phys. Rev. D **97**, 043506 (2018), arXiv:1707.03240 [astro-ph.CO].
[63] N. Bartolo *et al.*, JCAP **12**, 026 (2016), arXiv:1610.06481 [astro-ph.CO].
[64] A. A. Starobinsky, JETP Lett. **30**, 682 (1979).
[65] C. Badger, H. Duval, T. Fujita, S. Kuroyanagi, A. Romero-Rodríguez, and M. Sakellariadou, Phys.

Rev. D **110**, 084063 (2024).
[66] V. F. Mukhanov and G. V. Chibisov, JETP Lett. **33**, 532 (1981).
[67] L. P. Grishchuk, Zh. Eksp. Teor. Fiz. **67**, 825 (1974).
[68] V. Rubakov, M. Sazhin, and A. Veryaskin, Physics Letters B **115**, 189 (1982).
[69] L. Abbott and M. B. Wise, Nuclear Physics B **244**, 541 (1984).
[70] T. L. S. Collaboration, J. Aasi, B. P. Abbott, R. Abbott, T. Abbott, M. R. Abernathy, K. Ackley, C. Adams, T. Adams, P. Addesso, R. X. Adhikari, *et al.*, Classical and Quantum Gravity **32**, 074001 (2015).
[71] F. Acernese, M. Agathos, K. Agatsuma, D. Aisa, N. Allemandou, A. Allocca, J. Amarni, P. Astone, G. Balestri, G. Ballardin, *et al.*, Classical and Quantum Gravity **32**, 024001 (2014).
[72] T. Akutsu *et al.* (KAGRA), PTEP **2021**, 05A101 (2021), arXiv:2005.05574 [physics.ins-det].
[73] B. P. Abbott, R. Abbott, T. D. Abbott, M. R. Abernathy, F. Acernese, K. Ackley, C. Adams, T. Adams, P. Addesso, R. X. Adhikari, *et al.*, Living Reviews in Relativity **21** (2018), 10.1007/s41114-018-0012-9.
[74] R. Abbott, T. D. Abbott, S. Abraham, F. Acernese, K. Ackley, A. Adams, C. Adams, R. X. Adhikari, V. B. Adya, C. Affeldt, *et al.* (LIGO Scientific Collaboration, Virgo Collaboration, and KAGRA Collaboration), Phys. Rev. D **104**, 022004 (2021).
[75] R. Abbott, T. D. Abbott, S. Abraham, F. Acernese, K. Ackley, A. Adams, C. Adams, R. X. Adhikari, V. B. Adya, and C. Affeldt (LIGO Scientific Collaboration, Virgo Collaboration, and KAGRA Collaboration), Phys. Rev. D **104**, 022005 (2021).
[76] T. Callister, M. Fishbach, D. Holz, and W. Farr, Astrophys. J. Lett. **896**, L32 (2020), arXiv:2003.12152 [astro-ph.HE].
[77] K. Turbang, M. Lalleman, T. A. Callister, and N. van Remortel, Astrophys. J. **967**, 142 (2024), arXiv:2310.17625 [astro-ph.HE].
[78] M. Lalleman, K. Turbang, T. Callister, and N. van Remortel, (2025), arXiv:2501.10295 [astro-ph.HE].
[79] G. Cusin, I. Dvorkin, C. Pitrou, and J.-P. Uzan, Phys. Rev. Lett. **120**, 231101 (2018), arXiv:1803.03236 [astro-ph.CO].
[80] A. C. Jenkins, M. Sakellariadou, T. Regimbau, and E. Slezak, Phys. Rev. D **98**, 063501 (2018), arXiv:1806.01718 [astro-ph.CO].
[81] G. Capurri, A. Lapi, C. Baccigalupi, L. Boco, G. Scelfo, and T. Ronconi, JCAP **11**, 032 (2021), arXiv:2103.12037 [gr-qc].
[82] T. Regimbau, Res. Astron. Astrophys. **11**, 369 (2011), arXiv:1101.2762 [astro-ph.CO].
[83] A. I. Renzini and J. Golomb, Astron. Astrophys. **691**, A238 (2024), arXiv:2407.03742 [astro-ph.CO].
[84] M. Ebersold and T. Regimbau, `https://git.ligo.org/michael.ebersold/agwb-forecast` (2025), placeholder citation – to be updated.
[85] S. Drasco and E. E. Flanagan, Phys. Rev. D **67**, 082003 (2003), arXiv:gr-qc/0210032.
[86] A. G. Abac *et al.* (LIGO Scientific, VIRGO, KAGRA), (2025), arXiv:2508.18080 [gr-qc].
[87] A. G. Abac *et al.* (LIGO Scientific, VIRGO, KAGRA), (2025), arXiv:2508.18081 [gr-qc].
[88] LIGO Scientific, VIRGO, KAGRA Collaborations, (2025), arXiv:2508.18082 [gr-qc].
[89] LIGO Scientific, VIRGO, KAGRA Collaborations, (2025), arXiv:2508.18083 [astro-ph.HE].
[90] L. Barsotti, L. McCuller, M. Evans, and P. Fritschel, `https://dcc.ligo.org/LIGO-T1800042/public`.
[91] A. Rocchi *et al.*, "Public expected o5 virgo ranges and sensitivity curves," (2025), vIR-0797A-25.
[92] LIGO Scientific, VIRGO, KAGRA Collaborations, (in prep.).
[93] A. Matas and J. Romano, Physical Review D **103** (2021), 10.1103/PhysRevD.103.062003.
[94] J. Lawrence, K. Turbang, A. Matas, A. I. Renzini, N. van Remortel, and J. D. Romano, Phys. Rev. D **107**, 103026 (2023), arXiv:2301.07675 [gr-qc].
[95] R. Smith and E. Thrane, Phys. Rev. X **8**, 021019 (2018).
[96] R. Buscicchio, A. Ain, M. Ballelli, G. Cella, and B. Patricelli, Phys. Rev. D **107**, 063027 (2023), arXiv:2209.01400 [gr-qc].
[97] M. R. Sah and S. Mukherjee, (2023), arXiv:2307.06405 [gr-qc].
[98] A. Nishizawa, A. Taruya, K. Hayama, S. Kawamura, and M.-a. Sakagami, Phys. Rev. D **79**, 082002 (2009).
[99] K. Riles and J. Zweizig, `https://dcc.ligo.org/T2000384/public` (2021).
[100] A. Matas, I. Dvorkin, T. Regimbau, and A. Romero, `https://dcc.ligo.org/P2000546/public` (2021).
[101] LIGO Scientific, VIRGO, KAGRA Collaborations, (in prep.).
[102] A. I. Renzini, B. Goncharov, A. C. Jenkins, and P. M. Meyers, Galaxies **10** (2022), 10.3390/galaxies10010034.
[103] P. A. R. Ade *et al.* (Planck), Astron. Astrophys. **594**, A13 (2016), arXiv:1502.01589 [astro-ph.CO].
[104] A. I. Renzini, A. Romero-Rodriguez, C. Talbot, M. Lalleman, S. Kandhasamy, K. Turbang, S. Biscoveanu, K. Martinovic, P. Meyers, L. Tsukada, K. Janssens, D. Davis, A. Matas, P. Charlton, G. chin Liu, and I. Dvorkin, Astrophys. J. **952**, 25 (2023), arXiv:2303.15696 [gr-qc].
[105] A. I. Renzini, A. Romero-Rodriguez, C. Talbot, M. Lalleman, S. Kandhasamy, K. Turbang, S. Biscoveanu, K. Martinovic, P. Meyers, L. Tsukada, K. Janssens, D. Davis, A. Matas, P. Charlton, G. chin Liu, and I. Dvorkin, Journal of Open Source Software **9**, 5454 (2024).
[106] B. P. Abbott, R. Abbott, T. D. Abbott, M. R. Abernathy, F. Acernese, K. Ackley, C. Adams, T. Adams, P. Addesso, R. Adhikari, *et al.* (LIGO Scientific Collaboration and Virgo Collaboration), Phys. Rev. Lett. **118**, 121101 (2017).
[107] B. P. Abbott, R. Abbott, T. D. Abbott, S. Abraham, F. Acernese, K. Ackley, C. Adams, V. B. Adya, C. Affeldt, Agathos, *et al.* (LIGO Scientific and Virgo Collaboration), Phys. Rev. D **100**, 061101 (2019).
[108] B. Allen and J. D. Romano, Phys. Rev. D **59**, 102001 (1999).
[109] L. S. Finn, S. L. Larson, and J. D. Romano, Phys. Rev. D **79**, 062003 (2009), arXiv:0811.3582 [gr-qc].
[110] V. Mandic, E. Thrane, S. Giampanis, and T. Regimbau, Phys. Rev. Lett. **109**, 171102 (2012).
[111] G. Ashton *et al.*, Astrophys. J. Suppl. **241**, 27 (2019), arXiv:1811.02042 [astro-ph.IM].
[112] K. Janssens, M. Ball, R. M. S. Schofield, N. Christensen, R. Frey, N. van Remortel, S. Banagiri, M. W. Coughlin, A. Effler, M. Gołkowski, J. Kubisz, and M. Ostrowski, Phys. Rev. D **107**, 022004 (2023).

[113] T. Callister, A. S. Biscoveanu, N. Christensen, M. Isi, A. Matas, O. Minazzoli, T. Regimbau, M. Sakellariadou, J. Tasson, and E. Thrane, Phys. Rev. X **7**, 041058 (2017), arXiv:1704.08373 [gr-qc].

[114] B. P. Abbott *et al.*, Phys. Rev. D **93**, 112004 (2016), [Addendum: Phys.Rev.D 97, 059901 (2018)], arXiv:1604.00439 [astro-ph.IM].

[115] D. V. Martynov *et al.*, Phys. Rev. A **95**, 043831 (2017), arXiv:1702.03329 [physics.optics].

[116] L. Nuttall *et al.*, Class. Quant. Grav. **32**, 245005 (2015), arXiv:1508.07316 [gr-qc].

[117] B. P. Abbott *et al.* (LIGO Scientific, Virgo), Class. Quant. Grav. **35**, 065010 (2018), arXiv:1710.02185 [gr-qc].

[118] D. Davis *et al.* (LIGO), Class. Quant. Grav. **38**, 135014 (2021), arXiv:2101.11673 [astro-ph.IM].

[119] A. F. Brooks *et al.* (LIGO Scientific), Appl. Opt. **60**, 4047 (2021), arXiv:2101.05828 [physics.ins-det].

[120] J. C. Driggers *et al.* (LIGO Scientific), Phys. Rev. D **99**, 042001 (2019), arXiv:1806.00532 [astro-ph.IM].

[121] A. Buikema *et al.*, Phys. Rev. D **102**, 062003 (2020).

[122] M. Tse, H. Yu, *et al.*, Phys. Rev. Lett. **123**, 231107 (2019).

[123] P. Nguyen, R. M. S. Schofield, A. Effler, C. Austin, V. Adya, M. Ball, S. Banagiri, K. Banowetz, C. Billman, *et al.*, Classical and Quantum Gravity **38**, 145001 (2021).

[124] S. Soni, C. Austin, A. Effler, R. M. S. Schofield, G. Gonzlez, V. V. Frolov, J. C. Driggers, A. Pele, A. L. Urban, G. Valdes, R. Abbott, and T. L. S. Collaboration, Classical and Quantum Gravity **38**, 025016 (2020).

[125] I. Fiori, F. Paoletti, M. Tringali, K. Janssens, C. Karathanasis, A. Menndez-Vzquez, A. Romero-Rodrguez, R. Sugimoto, T. Washimi, V. Boschi, A. Chiummo, M. Cielar, R. De Rosa, C. Rossi, F. Di Renzo, I. Nardecchia, A. Pasqualetti, B. Patricelli, P. Ruggi, and N. Singh, Galaxies **8**, 82 (2020).

[126] F. Acernese *et al.* (Virgo Collaboration), Phys. Rev. Lett. **131**, 041403 (2023).

[127] F. Acernese, M. Agathos, L. Aiello, A. Allocca, A. Amato, S. Ansoldi, S. Antier, M. Arène, N. Arnaud, S. Ascenzi, *et al.* (Virgo Collaboration), Phys. Rev. Lett. **123**, 231108 (2019).

[128] F. Acernese, M. Agathos, L. Aiello, A. Ain, A. Allocca, A. Amato, S. Ansoldi, S. Antier, M. Arène, N. Arnaud, *et al.* (The Virgo Collaboration), Phys. Rev. Lett. **125**, 131101 (2020).

[129] F. Acernese *et al.* (Virgo), Class. Quant. Grav. **39**, 235009 (2022), arXiv:2203.04014 [gr-qc].

[130] F. Acernese *et al.* (Virgo), Class. Quant. Grav. **40**, 185006 (2023), arXiv:2210.15633 [gr-qc].

[131] E. Capote *et al.*, Phys. Rev. D **111**, 062002 (2025), arXiv:2411.14607 [gr-qc].

[132] W. Jia *et al.* (members of the LIGO Scientific†), Science **385**, 1318 (2024), arXiv:2404.14569 [gr-qc].

[133] S. Soni *et al.* (LIGO), Class. Quant. Grav. **42**, 085016 (2025), arXiv:2409.02831 [astro-ph.IM].

[134] A. Viets and M. Wade, *Subtracting Narrow-band Noise from LIGO Strain Data in the Third Observing Run*, Tech. Rep. LIGO-T2100058-v5 (LIGO Scientific Collaboration, 2021) lIGO Document Control Center: `https://dcc.ligo.org/LIGO-T2100058/public`.

[135] G. Vajente, Y. Huang, M. Isi, J. Driggers, J. Kissel, M. Szczepaczyk, and S. Vitale, Physical Review D **101** (2020), 10.1103/physrevd.101.042003.

[136] "LEMI-120," `https://lemisensors.com/?p=245`.

[137] (2025), arXiv:2508.18079 [gr-qc].

[138] K. Riles *et al.*, "Information on self-gating of $h(t)$ used in o3 continuous-wave and stochastic searches," (2020), t2000384-v4.

[139] A. Matas, I. Dvorkin, A. Romero, and T. Regimbau, "Application of gating to stochastic searches in o3," (2021), p2000546.

[140] D. J. A. McKechan, C. Robinson, and B. S. Sathyaprakash, Class. Quant. Grav. **27**, 084020 (2010), arXiv:1003.2939 [gr-qc].

[141] S. Karki *et al.*, Rev. Sci. Instrum. **87**, 114503 (2016), arXiv:1608.05055 [astro-ph.IM].

[142] C. Biwer, D. Barker, J. C. Batch, J. Betzwieser, R. P. Fisher, E. Goetz, S. Kandhasamy, S. Karki, J. S. Kissel, A. P. Lundgren, *et al.*, Phys. Rev. D **95**, 062002 (2017).

[143] A. G. Sullivan *et al.*, Phys. Rev. D **108**, 022003 (2023), arXiv:2304.01188 [astro-ph.IM].

[144] E. Thrane, N. Christensen, and R. M. S. Schofield, Physical Review D **87** (2013), 10.1103/physrevd.87.123009.

[145] E. Thrane, N. Christensen, R. Schofield, and A. Effler, Physical Review D **90** (2014), 10.1103/physrevd.90.023013.

[146] M. W. Coughlin, A. Cirone, P. Meyers, S. Atsuta, V. Boschi, A. Chincarini, N. L. Christensen, R. De Rosa, A. Effler, I. Fiori, *et al.*, Physical Review D **97** (2018), 10.1103/physrevd.97.102007.

[147] W. O. Schumann, Zeitschrift Naturforschung Teil A **7**, 149 (1952).

[148] W. O. Schumann, Zeitschrift Naturforschung Teil A **7**, 250 (1952).

[149] K. Janssens *et al.*, Phys. Rev. D **107**, 022004 (2023), arXiv:2209.00284 [gr-qc].

[150] E. Thrane and J. D. Romano, Physical Review D **88**, 124032 (2013).

[151] L. Sun *et al.*, Class. Quant. Grav. **37**, 225008 (2020), arXiv:2005.02531 [astro-ph.IM].

[152] L. Sun *et al.*, (2021), arXiv:2107.00129 [astro-ph.IM].

[153] S. Vitale, C.-J. Haster, L. Sun, B. Farr, E. Goetz, J. Kissel, and C. Cahillane, Phys. Rev. D **103**, 063016 (2021).

[154] J. Yousuf, S. Kandhasamy, and M. A. Malik, Phys. Rev. D **107**, 102002 (2023), arXiv:2301.13531 [gr-qc].

[155] T. W. B. Kibble, J. Phys. A **9**, 1387 (1976).

[156] S. Sarangi and S. H. H. Tye, Phys. Lett. B **536**, 185 (2002), arXiv:hep-th/0204074.

[157] T. Damour and A. Vilenkin, Phys. Rev. D **71**, 063510 (2005), arXiv:hep-th/0410222.

[158] X. Siemens, V. Mandic, and J. Creighton, Phys. Rev. Lett. **98**, 111101 (2007).

[159] M. S. Turner, Phys. Rev. D **55**, R435 (1997).

[160] R. Bar-Kana, Phys. Rev. D **50**, 1157 (1994).

[161] T. Regimbau, Research in Astronomy and Astrophysics **11**, 21 (2011).

[162] C. Périgois, C. Belczynski, T. Bulik, and T. Regimbau, Phys. Rev. D **103**, 043002 (2021), arXiv:2008.04890 [astro-ph.CO].

[163] J. M. Ezquiaga and D. E. Holz, Astrophys. J. Lett. **909**, L23 (2021), arXiv:2006.02211 [astro-ph.HE].

[164] S. Marassi, R. Schneider, and V. Ferrari, Mon. Not. Roy. Astron. Soc. **398**, 293 (2009), arXiv:0906.0461 [astro-ph.CO].

[165] P. M. Meyers, K. Martinovic, N. Christensen, and M. Sakellariadou, Phys. Rev. D **102**, 102005 (2020).
[166] B. P. Abbott *et al.* (LIGO Scientific, Virgo), Phys. Rev. Lett. **116**, 131102 (2016), arXiv:1602.03847 [gr-qc].
[167] R. Abbott, T. D. Abbott, S. Abraham, F. Acernese, K. Ackley, *et al.* (The LIGO Scientific Collaboration and the Virgo Collaboration), The Astrophysical Journal Letters **913**, L7 (2021).
[168] R. Abbott, T. D. Abbott, F. Acernese, K. Ackley, C. Adams, *et al.* (The LIGO Scientific Collaboration, Virgo Collaboration, and KAGRA Collaboration), arXiv:2111.03634 (2022).
[169] E. S. Phinney, (2001), arXiv:astro-ph/0108028.
[170] X.-J. Zhu, E. Howell, T. Regimbau, D. Blair, and Z.-H. Zhu, Astrophys. J. **739**, 86 (2011), arXiv:1104.3565 [gr-qc].
[171] P. A. Rosado, Phys. Rev. D **84**, 084004 (2011), arXiv:1106.5795 [gr-qc].
[172] X.-J. Zhu, E. Howell, T. Regimbau, D. Blair, and Z.-H. Zhu, Astrophys. J. **739**, 86 (2011), arXiv:1104.3565 [gr-qc].
[173] K. Martinovic, C. Perigois, T. Regimbau, and M. Sakellariadou, Astrophys. J. **940**, 29 (2022), arXiv:2109.09779 [astro-ph.SR].
[174] V. Mandic, S. Bird, and I. Cholis, Phys. Rev. Lett. **117**, 201102 (2016), arXiv:1608.06699 [astro-ph.CO].
[175] S. Mukherjee and J. Silk, Mon. Not. Roy. Astron. Soc. **506**, 3977 (2021), arXiv:2105.11139 [gr-qc].
[176] G. Pratten, S. Husa, C. Garcia-Quiros, M. Colleoni, A. Ramos-Buades, H. Estelles, and R. Jaume, Phys. Rev. D **102**, 064001 (2020), arXiv:2001.11412 [gr-qc].
[177] G. Pratten *et al.*, Phys. Rev. D **103**, 104056 (2021), arXiv:2004.06503 [gr-qc].
[178] A. Abac, T. Dietrich, A. Buonanno, J. Steinhoff, and M. Ujevic, Phys. Rev. D **109**, 024062 (2024), arXiv:2311.07456 [gr-qc].
[179] M. Colleoni, F. A. Ramis Vidal, N. K. Johnson-McDaniel, T. Dietrich, M. Haney, and G. Pratten, Phys. Rev. D **111**, 064025 (2025), arXiv:2311.15978 [gr-qc].
[180] T. Dietrich, A. Samajdar, S. Khan, N. K. Johnson-McDaniel, R. Dudi, and W. Tichy, Phys. Rev. D **100**, 044003 (2019), arXiv:1905.06011 [gr-qc].
[181] M. Fishbach, D. E. Holz, and W. M. Farr, The Astrophysical Journal **863**, L41 (2018).
[182] M. Dominik, K. Belczynski, C. Fryer, D. E. Holz, E. Berti, T. Bulik, I. Mandel, and R. O'Shaughnessy, Astrophys. J. **779**, 72 (2013), arXiv:1308.1546 [astro-ph.HE].
[183] M. Mapelli, N. Giacobbo, E. Ripamonti, and M. Spera, Mon. Not. Roy. Astron. Soc. **472**, 2422 (2017), arXiv:1708.05722 [astro-ph.GA].
[184] F. Santoliquido, M. Mapelli, Y. Bouffanais, N. Giacobbo, U. N. Di Carlo, S. Rastello, M. C. Artale, and A. Ballone, Astrophys. J. **898**, 152 (2020), arXiv:2004.09533 [astro-ph.HE].
[185] M. Mapelli, Y. Bouffanais, F. Santoliquido, M. A. Sedda, and M. C. Artale, Mon. Not. Roy. Astron. Soc. **511**, 5797 (2022), arXiv:2109.06222 [astro-ph.HE].
[186] X.-X. Kou, G. Fragione, and V. Mandic, Phys. Rev. D **109**, 123036 (2024), arXiv:2401.04347 [gr-qc].
[187] The LIGO Scientific Collaboration, Virgo Collaboration, and KAGRA Collaboration, "Noise curves used for simulations in the update of the observing scenarios paper," LIGO Document Control Center entry T2000012 (2022).
[188] R. Abbott, T. D. Abbott, F. Acernese, K. Ackley, C. Adams, *et al.* (The LIGO Scientific Collaboration, Virgo Collaboration, and KAGRA Collaboration), arXiv:2111.03606 (2021).
[189] P. Ajith, M. Hannam, S. Husa, Y. Chen, B. Brgmann, *et al.*, Physical Review Letters **106**, 241101 (2011).
[190] P. Madau and T. Fragos, Astrophys. J. **840**, 39 (2017), arXiv:1606.07887 [astro-ph.GA].
[191] L. Lehoucq, I. Dvorkin, and L. Rezzolla, (2025), arXiv:2503.20877 [astro-ph.HE].
[192] R. Abbott *et al.* (The LIGO Scientific Collaboration, and Virgo Collaboration), Astrophys. J. **896**, L44 (2020).
[193] R. Abbott *et al.* (LIGO Scientific, KAGRA, VIRGO), Astrophys. J. Lett. **915**, L5 (2021), arXiv:2106.15163 [astro-ph.HE].
[194] A. G. Abac *et al.* (LIGO Scientific, Virgo, KAGRA, VIRGO), Astrophys. J. Lett. **970**, L34 (2024), arXiv:2404.04248 [astro-ph.HE].
[195] F. Foucart, L. Buchman, M. D. Duez, M. Grudich, L. E. Kidder, I. MacDonald, A. Mroue, H. P. Pfeiffer, M. A. Scheel, and B. Szilagyi, Phys. Rev. D **88**, 064017 (2013), arXiv:1307.7685 [gr-qc].
[196] F. Pannarale, E. Berti, K. Kyutoku, B. D. Lackey, and M. Shibata, Phys. Rev. D **92**, 081504 (2015), arXiv:1509.06209 [gr-qc].